



HAL
open science

Robust Mesoporous CoMo/ γ -Al₂O₃ Catalysts from Cyclodextrin-Based Supramolecular Assemblies for Hydrothermal Processing of Microalgae: Effect of the Preparation Method

Rudina Bleta, Benedetto Schiavo, Natale Corsaro, Paula Costa, Alberto Giaconia, Leonardo Interrante, Eric Monflier, Giuseppe Pipitone, Anne Ponchel, Salvatore Sau, et al.

► To cite this version:

Rudina Bleta, Benedetto Schiavo, Natale Corsaro, Paula Costa, Alberto Giaconia, et al.. Robust Mesoporous CoMo/ γ -Al₂O₃ Catalysts from Cyclodextrin-Based Supramolecular Assemblies for Hydrothermal Processing of Microalgae: Effect of the Preparation Method. ACS Applied Materials & Interfaces, 2018, 10 (15), pp.12562 - 12579. 10.1021/acsami.7b16185 . hal-01787235

HAL Id: hal-01787235

<https://hal.science/hal-01787235>

Submitted on 13 Nov 2023

HAL is a multi-disciplinary open access archive for the deposit and dissemination of scientific research documents, whether they are published or not. The documents may come from teaching and research institutions in France or abroad, or from public or private research centers.

L'archive ouverte pluridisciplinaire **HAL**, est destinée au dépôt et à la diffusion de documents scientifiques de niveau recherche, publiés ou non, émanant des établissements d'enseignement et de recherche français ou étrangers, des laboratoires publics ou privés.

Robust Mesoporous CoMo/ γ -Al₂O₃ Catalysts from Cyclodextrin-based Supramolecular Assemblies for Hydrothermal Processing of Microalgae: Effect of the Preparation Method

*Rudina Bleta,^{*a} Benedetto Schiavo,^b Natale Corsaro,^c Paula Costa,^d Alberto Giaconia,^c Leonardo Interrante,^b Eric Monflier,^a Giuseppe Pipitone,^{a,b} Anne Ponchel,^a Salvatore Sau,^c Onofrio Scialdone,^b Sébastien Tilloy^a and Alessandro Galia^{*b}*

^a. Univ. Artois, CNRS, Centrale Lille, ENSCL, Univ. Lille, UMR 8181, Unité de Catalyse et de Chimie du Solide (UCCS) F-62300 Lens, France. Email : rudina.bleta@univ-artois.fr

^b. Dipartimento del l'Innovazione Industriale e Digitale-Ingegneria Chimica, Gestionale, Informatica, Meccanica (DIID) Università di Palermo Viale delle Scienze, Ed 6, 90128 Palermo, Italy. Email: alessandro.galia@unipa.it

^c. ENEA-Casaccia Research Center Via Anguillarese 301, I-00123, Rome, Italy

^d. Laboratório Nacional de Energia e Geologia (LNEG) Estrada do Paço do Lumiar, 22, 1649-038 Lisbon, Portugal

Keywords: heterogeneous catalysts, microalgae, hydrothermal liquefaction, cyclodextrin, biocrude

ABSTRACT

Hydrothermal liquefaction (HTL) is a promising technology for the production of biocrude oil from microalgae. Although this catalyst-free technology is efficient under high-temperature and high-pressure conditions, the biocrude yield and quality can be further improved by using heterogeneous catalysts. The design of robust catalyst that preserve their performance under hydrothermal conditions will be therefore very important in the development of biorefinery technologies. In this work, we describe two different synthetic routes, *i.e.* impregnation and cyclodextrin-assisted one-pot colloidal approach, for the preparation in aqueous phase of six high surface area CoMo/ γ -Al₂O₃ catalysts. Catalytic tests performed on HTL of *Nannochloropsis gaditana* microalga indicate that solids prepared by the one-pot colloidal approach show higher hydrothermal stability and enhanced biocrude yield with respect to the catalyst-free test. The positive effect of the substitution of the block copolymer Tetronic T90R4 for Pluronic F127 in the preparation procedure was evidenced by diffuse reflectance UV-visible spectroscopy, X-ray diffraction, N₂-adsorption-desorption and H₂-temperature programmed reduction measurements and confirmed by the higher quality of the obtained biocrude, which exhibited lower oxygen content and higher energy recovery equal to 62.5% of the initial biomass.

Introduction

The development of heterogeneously catalyzed processes for the conversion of biomass in aqueous phase is a challenge for biorefinery technologies, in concert with replacement of traditional fossil fuels feedstocks.^{1,2} Among biomass, microalgae have a significant potential as suitable renewable feedstock owing to their high production rate achievable in open ponds or photobioreactors and their interesting energy content related to the presence of lipids, in addition

to proteins and carbohydrates.³ One of the most promising conversion routes toward the processing of the entire algal feedstock is the hydrothermal liquefaction (HTL) which is carried out in water, under high temperature (250-550 °C) and high pressure (10-25 MPa) conditions⁴ producing bio-oil (or biocrude) as main product.⁵⁻⁹ A key advantage of this process is that at near critical or supercritical conditions, water behaves as non-polar solvent due to the decreased value of the dielectric constant (ϵ), thus allowing ease solubilization of the biomass compounds. Moreover, as the ionic product of water (K_w) increases with temperature, changing from 10^{-14} to 10^{-11} in the range of 25-350 °C, water behaves also as acid catalyst for hydrolysis reactions involving carbohydrates and lipids.¹⁰ The biocrudes produced by HTL processes are generally more viscous and have higher oxygen contents than conventional crude oil.¹¹ In order to meet the requirements of biofuel standards, biocrude must be upgraded by hydrodeoxygenation processes.¹² Therefore the development of hydrothermally stable catalysts that could be added during the HTL of microalgae to decrease the oxygen content of the obtained biocrude would be interesting.

The first extensive work on the catalytic HTL of microalgae *Nannochloropsis* at 350 °C was presented by Duan and Savage¹³ who showed that the bio-oil yield could be increased by using both noble metals (Pd, Pt and Ru) supported on carbon (metal loading 5 wt%) and less expensive transition metals such as Ni, Co and Mo supported on alumina, silica or a zeolite. It was found that the utilization of a high amount of catalyst (50 wt% with respect to the dry and ash free algae) could increase the bio-oil yield, while decreasing its apparent viscosity. However, the structural transformations of the composite materials exposed to hydrothermal conditions were not evaluated. Pt and Pd addition was also confirmed to increase the bio-oil yield with *Chlorella pyrenoidosa*¹⁴ at lower temperatures (240 °C and 280 °C) when supported on Al₂O₃, while only Pt was effective with *Chlorella vulgaris* at 350 °C¹⁵. Ni, Fe and Ce were also deposited on a high

surface area zeolite (HZSM-5) and they were shown to increase the content of aromatics and alkanes and reduce oxygenated and nitrogenated compounds in the bio-oil obtained from HTL of the marine microalga *Laminaria Japonica*¹⁶ or from *Chlorella pyrenoidosa*.¹⁷ Very recently, Egesa *et al.*¹⁸ showed that ferrite magnetic nanoparticles doped with Zn and Mg could increase the biocrude yield in the liquefaction of *Spirulina* by 13.9%, while the percentages of heteroatom compounds, nitrogen and oxygen were significantly reduced. Moreover, the Zn-doped ferrite nanoparticles were easily recovered with a separation efficiency of 99% and recycled to further catalyze the HTL process. In another recent critical review, Galadima *et al.*¹⁹ documented the use of different heterogeneous catalysts in the liquefaction of several algae species. An extensive overview of the literature was provided on the potential beneficial effects of these solids in both liquefaction and bio-oil upgrading.

On the other hand, Ravenelle *et al.*,^{20,21} found that commercial γ -Al₂O₃-supported catalysts were more stable in biomass solutions than when they were in pure water at elevated temperature and pressure. This result was later explained by the stabilizing effect of polyols which form strongly bound multidentate alkoxy species on the γ -Al₂O₃ surface, stabilizing it against transformation to boehmite in hot water.²² As stated by Weckhuysen *et al.*²³ the stability of commercial Pt/ γ -Al₂O₃ can also be affected by lignin-derived aromatic oxygenates which tend to adsorb on the support surface by coordinating *via* the oxygen functionalities, thus protecting the support against structural transformations under liquid phase reforming reaction conditions.

Although these studies have provided important insights into the stability of γ -Al₂O₃-supported catalysts in hot water, there are currently no investigations on how the preparation method may affect both the catalytic performance and the hydrothermal stability of these solids in the liquefaction of microalgae. A compromise between these two aspects must be found in order to

maximize the recovery of microalgae energy and its densification and storage in the form of bio-oil.

Cyclodextrins (CDs) are water soluble cyclic oligosaccharides composed of n glucose units. They possess a hydrophobic internal cavity and a hydrophilic exterior surface with a large number of hydroxyl groups. The most common cyclodextrins are α -CD, β -CD and γ -CD composed respectively of 6, 7 and 8 glucose units in the ring. Cyclodextrins demonstrate multifunctional properties such as the ability to form supramolecular adducts or host-guest inclusion complexes with a large number of molecules of appropriate size and shape.^{24,25} Moreover, these cyclic oligosaccharides have also the unusual ability to form supramolecular assemblies with a large variety of polymers and metal salts, and this property offers interesting possibilities for the preparation of metal-capped porous composites for applications in heterogeneous catalysis and photocatalysis.^{26,27}

In this work, we compare two different preparation methods to fabricate CoMo/ γ -Al₂O₃ catalysts with suitable structural and textural characteristics and high chemical stability under hydrothermal conditions. The supramolecular assemblies formed between the randomly methylated- β -cyclodextrin (RaMe β -CD) and two block copolymers (Pluronic F127 and Tetronic T90R4) are used as template to prepare a highly porous γ -Al₂O₃ network over which uniform dispersion of the metal oxide nanoparticles can be achieved. The catalytic performance of these mesoporous solids is evaluated in the hydrothermal liquefaction of *Nannochloropsis gaditana* microalga. Biocrude oil is analyzed by elemental analysis and gas chromatography-mass spectrometry (GC-MS), while the gas phase composition is determined by GC. To the best of our knowledge, this is the first study reporting the effect of the preparation method on the catalytic performance of mesoporous CoMo/ γ -Al₂O₃ for the hydrothermal liquefaction of microalgae. In addition, we investigate the

chemical stability of these solids under hydrothermal conditions, in view of proposing guidelines that might be useful in practice for the selection of the appropriate catalyst for the HTL of microalgae or other biomass feedstocks.

Experimental Section

Chemicals

Both the linear poloxamer Pluronic F127 with a chemical formula $\text{PEO}_{106}\text{PPO}_{70}\text{PEO}_{106}$ [PEO = poly(ethylene oxide) and PPO = poly(propylene oxide)] (Mw 12500 g/mol) and the star-shaped poloxamine Tetronic T90R4 (ethylenediamine tetrakis (ethoxylate-block-propoxylate) tetrol) with a chemical formula $(\text{PPO}_{19}\text{PEO}_{16})_2\text{NCH}_2\text{CH}_2\text{N}(\text{PPO}_{19}\text{PEO}_{16})_2$ (Mw 7200 g/mol) were purchased from Sigma Aldrich. Randomly methylated β -cyclodextrin (denoted RaMe β -CD, average degree of molar substitution (DS) of 1.8 and average Mw 1310 g/mol) and native β -cyclodextrin (denoted β -CD, average Mw 1135 g/mol) were gifts from Wacker Chemie GmbH and Roquette Frères respectively. Aluminum tri-sec-butoxide, $\text{Al}[\text{OCH}(\text{CH}_3)\text{C}_2\text{H}_5]_3$ (referred to as ASB, Mw 246.32 g/mol), (HNO_3 , 68 wt%), cobalt (II) nitrate hexahydrate $\text{Co}(\text{NO}_3)_2 \cdot 6\text{H}_2\text{O}$ (Mw 291.03 g/mol) and ammonium heptamolybdate tetrahydrate $(\text{NH}_4)_6\text{Mo}_7\text{O}_{24} \cdot 4\text{H}_2\text{O}$ (Mw 1235.86 g/mol) were procured from Sigma-Aldrich. The microalga *Nannochloropsis gaditana* was purchased from Algaspring in powder form. The proximate analysis of the used microalgae batch was provided by the supplier. Ultrapure water HPLC grade was purchased from VWR International. Cyclohexane and acetone (analytical grade) were purchased from Sigma-Aldrich. Nitrogen and helium gas (99.999% purity) were obtained from Air Liquide. All chemicals were used as received, without further purification.

Preparation of mesoporous γ - Al_2O_3 supports and CoMo/ γ - Al_2O_3 catalysts

Mesoporous γ -Al₂O₃ supports were prepared using block copolymer/RaMe β -CD supramolecular assemblies as template and boehmite (AlO(OH)) nanoparticles as building blocks. Boehmite nanoparticles were synthesized in aqueous phase according to a previously reported sol-gel method.²⁸ Typically, in a dry 250 mL flask, 185 mL of hot distilled water (85 °C) was added fast to 25.3 g (0.1 mol) of ASB at a hydrolysis ratio of 100 (h = H₂O/Al). After 15 min, the hydroxide precipitate was peptized by adding dropwise 0.474 mL (0.1 mol) of HNO₃ ([HNO₃]/[Al] = 0.07). The mixture was maintained under reflux at 85 °C for 24 h. The final product was a transparent suspension of boehmite nanoparticles (pH 4.4-4.8) with an aluminum concentration of 0.486 mol/L. 80 mL aliquots of the above colloidal solution were then mixed with a block copolymer solution (3 wt% Pluronic F127, EO/Al molar ratio = 1) and a RaMe β -CD one (80 mg/mL RaMe β -CD, RaMe β -CD/Al molar ratio = 0.126). Hydrosols were maintained under stirring for 3 h, then allowed to equilibrate at 25 °C for additional 24 h. After drying at 60 °C, xerogels were calcined in air at 500 °C for 4 h with a heating ramp of 5 °C/min.

For the preparation of γ -Al₂O₃ supported bimetallic CoMo catalysts, two different synthetic procedures were used, *i.e.* the impregnation method and the direct incorporation (also referred to as one-pot colloidal approach). The appropriate amount of Co(NO₃)₂·6H₂O and (NH₄)₆Mo₇O₂₄·4H₂O was used in both preparation methods in order to obtain 0.6-1.2 wt% Co and 6.4-15.7 wt% Mo in the final catalysts.

In the first method, 500 mg of the calcined mesoporous γ -Al₂O₃ prepared using RaMe β -CD/Pluronic F127 assemblies as template were impregnated at pH 5 first with a Mo/ β CD aqueous solution, then with a Co/ β CD one (total volume 5 mL, Mo(Co)/ β CD molar ratio = 60). Suspensions were maintained under stirring at 75 °C until the water was completely evaporated, and then dried at 120 °C for 24 h. Two successive calcinations were performed at 500 °C for 2 h under air flow,

the first one after molybdenum addition and the second one after cobalt addition. The catalysts prepared by impregnation are labelled CoMo1, CoMo2 and CoMo3. CoMo1 and CoMo2 contain identical loadings in active metals (*i.e.* 0.6 wt% Co and 6.4 wt% Mo), while higher metal loadings were used for the preparation of CoMo3 (*i.e.* 1.2 wt% Co and 15.7 wt% Mo). The difference between CoMo1 and CoMo2 resides in the order of introduction of $\text{Co}(\text{NO}_3)_2 \cdot 6\text{H}_2\text{O}$ and $(\text{NH}_4)_6\text{Mo}_7\text{O}_{24} \cdot 4\text{H}_2\text{O}$ (see Table 1). In the second method, 20 mL aliquots of the boehmite sol were mixed with 20 mL aliquots of CoMo/RaMe β -CD/F127 (CoMo4 and CoMo5) or CoMo/RaMe β -CD/T90R4 (CoMo6) metallo-supramolecular assemblies (EO/Al = 1 and RaMe β -CD/Al = 0.126). The difference between CoMo4 and CoMo5 concerns the loadings in active elements (*i.e.* 0.6 wt% Co and 6.4 wt% Mo for CoMo4, and 1.2 wt% Co and 15.7 wt% Mo for CoMo5). On the other hand, CoMo5 and CoMo6 contain the same loadings in active elements (*i.e.* 1.2 wt% Co and 15.7 wt% Mo), but their difference resides on the polymer used as template in the preparation method. Thus, CoMo5 was prepared using Pluronic F127 as template, while CoMo6 was prepared using Tetronic 90R4 (see Table 1).

Hydrothermal conversion tests of microalgae and characterization of the products

A commercial AISI 316L Swagelok VCR male connector (1 inch nominal diameter), closed by two VCR caps with silver plated AISI 316L-stainless steel disposable gaskets, was used as reactor with a volume of 29.7 mL. One of the cap was equipped with a 1/16" male connector to couple the vessel to an expansion chamber through a 1/16" OD tube. This chamber with known volume (18 mL) was equipped with valves to purge, evacuate and isolate it from the reactor, and with a pressure transducer (Honeywell) for pressure measurement. The chamber was used as gas collection system (GCS) to collect and quantify the amount of gas phase in the reactor at the end of each test. The GCS was equipped with a gas sampling system closed by a rubber septum to

collect the gas phase with a gas-tight syringe. The gas samples were analyzed by gas chromatography (GC) to determine the composition of the gas. In a typical experiment, 1 g of dry microalga and 8.9 g of HPLC grade water were loaded in the reactor, so that 30% of the reactor volume was filled with an aqueous biomass slurry 10 wt%. The prepared catalysts were added in 80 mg amount. Then the reactor was manually closed without sealing it, and purged with nitrogen at 0.2-0.3 MPa in order to remove the air. Nitrogen was introduced in the reactor from the GCS which was purged as well. After 5 min flushing, the reactor was sealed and the two connected systems (reactor and GCS) were further purged with nitrogen performing 5 cycles of pressurization at 1.6 MPa and pressure release up to 0.25 MPa. At the end of this procedure the systems were left with a residual nitrogen atmosphere at 0.25 MPa and disconnected from the GCS. The gas phase remained in the GCS was sampled and analyzed by GC to control that oxygen had been effectively removed by this procedure.

The reactor was then inserted in a modified GC oven HP G1540A apparatus whose temperature is electronically controlled. The oven temperature was initially set at 30 °C for 10 minutes to equilibrate the reactor then the temperature of the oven was set to 449 °C and, after 18.3 minutes, the set point was changed to 377 °C and kept at this value for the selected reaction time (15 min). This temperature profile of the oven corresponded to an increase of the temperature inside the reactor with a heating rate of about 19 °C/min up to the reaction temperature of 375 °C, which was then hold for the desired reaction time. After 15 min, the reactor was quickly cooled down by immersion in water at ambient temperature to stop the chemical evolution of the system, then the reactor was left for one hour in vertical position for gravity separation of the products inside. Then the reactor was reconnected with the GCS with the reactor valve still closed. The GCS assembly was evacuated through vacuum/purge outlet shown in Figure 1, and the gas phase inside the reactor

was expanded in the GCS by opening the reactor valve. The pressure value of the expanded gas was measured and used to calculate the amount of gas phase using the ideal gas law. To perform analysis of the composition of the gas, the GCS valve (Figure 1) was closed, and the reactor was disconnected from the GCS. At least, four gas samples were collected with a syringe through the rubber septum of the GCS and injected into the GC for the analysis of the composition.

After the disconnection from the GCS, the reactor was opened and the liquid and solid products were collected and separated. First the aqueous phase was poured from the reactor into a vacuum filtering system equipped with 47 mm diameter nylon membrane filter (Alltech) with 0.2 μm average pore size. The bio-crude was too viscous to flow out of the vessel and it was recovered by three consecutive extractions with 15 mL of cyclohexane; the organic liquid solution was vacuum filtered through the nylon membrane with the same features previously reported. A fourth extraction with solvent was performed by sonicating the reactor for ten minutes. The filtered cyclohexane with the extracted bio-oil contained also some entrained water which separated by gravity in the bottom of the flask. The cyclohexane solution with the extracted bio-oil was transferred into a 100 mL pre-weighted flask, while residual water (mixed with the remaining small amount of the cyclohexane-solution) was transferred in a centrifugation glass tube.

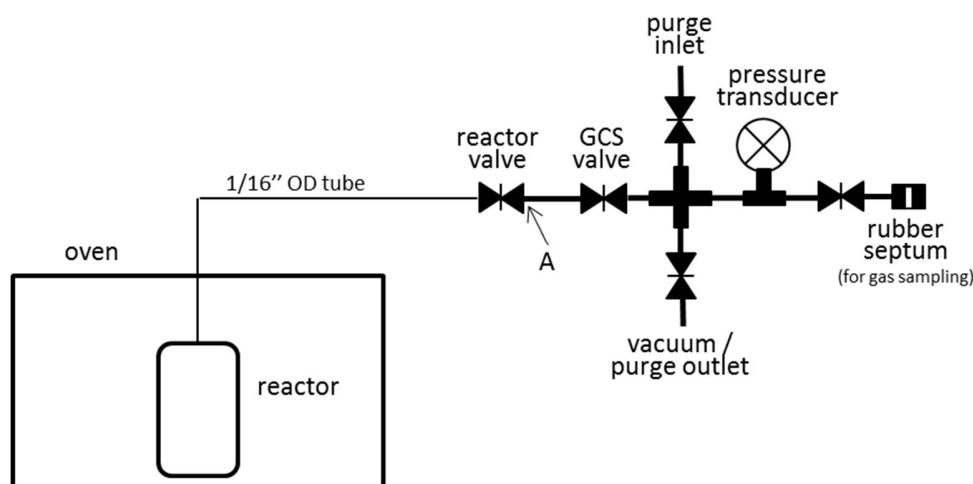


Figure 1. Scheme of the experimental apparatus. After the reaction and the cooling, the reactor is connected to the gas collection system (GCS) assembly through the connection indicated by “A”.

All the operations performed with the cyclohexane, except for the centrifugation, were then repeated by using acetone as solvent to extract the residual bio-oil and complete its recovery from the vessel. The organic-aqueous mixture contained in the centrifugation glass tube was centrifuged at 3000 rpm for 10 minutes, after this time the two phases were well separated. The aqueous phase was recovered with a syringe and added to the main aqueous phase previously collected by filtration procedure and stored into a pre-weighted 10 mL vial, while the organic phase was merged with the biocrude-cyclohexane solution. The water-soluble products were determined after drying the content of the 10 mL vial at 60 °C overnight. The solid products were determined after drying the filter with the remaining solid residue cake at 105 °C. The drying time ranged between 4 and 8 hours. Drying was considered complete when the mass of the filter with solid residue reached a stable value in two consecutive determinations. Both cyclohexane and acetone used to solubilize the biocrude oil were removed by evaporation under reduced pressure in a BUCHI RII rotavapor. The evaporation of the solvent was continued at room temperature under fume hood and was considered as completed when the flask reached constant weight (± 0.5 mg). The mass yield of each phase was evaluated with respect to the initial mass of dry microalgae (dry biomass basis). Selected tests were repeated three-four times to check reproducibility. The bio-oil yield was obtained with a standard deviation lower than ± 2 %.

Hydrothermal test for the catalyst stability

Catalysts were exposed to the same operative conditions used to convert the microalgae (*i.e.* 375 °C for 15 min), but without the presence of biomass inside the reactor. In this case, a stainless steel

cylinder was put inside the reactor to host the catalyst and to facilitate its recovery at the end of the test. After the test, the cylinder was placed in a stove at 60 °C for 12 h to remove the water, and then the treated catalyst was recovered and analyzed.

Analytical methods

Dynamic light scattering (DLS) measurements were carried out on a Malvern Zeta Nanosizer at a scattering angle (θ) of 173° (backscattering detection). The instrument was equipped with a 4 mW He-Ne laser operating at 633 nm. The temperature was varied between 25 and 50 °C and controlled to within $\pm 0.1^\circ\text{C}$. Samples were analyzed immediately after preparation or two months later. Diffuse Reflectance (DR) UV-visible spectra were collected on solid catalysts using a Perkin Elmer (Lambda 19) spectrophotometer equipped with an integrating sphere. Samples were placed in quartz cells and BaSO₄ was used as the reference. For the aqueous CoMo solutions, UV-Visible measurements were performed using the same apparatus in normal mode. X-ray powder diffraction patterns were recorded on a Siemens D5000 X-ray diffractometer in a Bragg-Brentano configuration operating with a Cu K α radiation ($\lambda = 1.5406 \text{ \AA}$). Scans were run between 10-30° and 50-70° 2 θ with a step size of 0.05° and a scan speed of 3 s. Nitrogen adsorption-desorption isotherms were collected at -196 °C using an adsorption analyzer Micromeritics Tristar 3020. Prior to analysis, 100-200 mg samples were outgassed at 320 °C overnight to remove the species adsorbed on the surface. From N₂-adsorption isotherms, specific surface areas were determined using the BET method²⁹ and pore size distributions were calculated using the BJH (Barrett, Joyner and Halenda) method.³⁰ Hydrogen temperature programmed reduction (H₂-TPR) measurements were carried out on a Micromeritics AutoChem 2920 chemisorption analyzer. Typically, 30-40 mg of calcined sample was introduced in a U-tube quartz reactor and outgassed under argon flow at 120 °C for at least 2 h. Then, a mixture of 5% H₂/Ar (v/v) was introduced into the sample reactor

at a flow rate of 10 mL/min. The sample was heated at 1000 °C with a ramp of 10 °C/min and maintained at that temperature for 30 minutes. The H₂ consumption during the reduction process was recorded using a thermal conductivity detector (TCD). The composition of the gas obtained in the experiments of HTL of microalgae was determined using a GC Agilent 7890B equipped with a Carboxen® 1000 60-80 mesh packed column from Supelco. Samples of 250 µL were injected through injector used in splitless mode and heated at 120 °C. A TCD detector was used with temperature at 275 °C. The oven was kept isothermal at 35 °C for 5 minutes, then it was heated up to 225 °C with an heating rate of 20 °C/min and kept isothermal for other 40 min. Helium (99.999% purity) was used as carrier gas with a flow rate of 30 mL/min. Elemental analyses were performed using a Thermo Finnigan - CE Instruments Flash EA 1112 analyzer and according to ISO 16948:2015 procedure “Solid biofuels - Determination of total content of carbon, hydrogen and nitrogen”. HHV of the obtained biocrude was calculated from the elemental analysis, according to the Boie’s formula³¹:

$$\text{HHV (MJ/kg)} = 0.3517C + 1.1626H - 0.111O + 0.1047S$$

were C, H, O, S are the weight percentages of the element in the sample. The Boie’s formula was also used for the estimation of the energy content of the algae, which resulted equal to 20 MJ/kg. This value was confirmed also by measurements performed with a bomb calorimeter (Parr, model 6200). The biocrude samples were also analyzed by GC-MS with the following procedure: around 20 mg were placed into a glass vial and 1.5 mL of acetone (Fluka, chromatography grade) were added. The solution was centrifuged (2000 rpm), and 50 µL were taken and diluted up to 1 mL with dichloromethane (Fluka, chromatography grade). An Agilent 7890 GC was used equipped with MS quadrupole 5973N and CP-Sil 8CB column (0.25mm x 30 m x 0.25 µm). Helium (99.9999% purity) was used as carrier gas with 1 mL/min flow rate. The oven temperature program

was 70 °C for 7 min, 70-280 °C ramp at 10 °C/min, 280 °C for 10 min. Temperatures of injector and of the interface GC-MS were 280 °C and 250 °C respectively. The MS detector was used in TIC modality (30-300 m/z); in order to obtain qualitative information, a NIST008 MS library was used for the spectra identification. The chromatography standards for the six quantified fatty acids (FAs), were purchased as follows: stearic acid (C18:0, $\geq 98.5\%$) by Sigma-Aldrich, oleic (C18:1, $\geq 99.0\%$) and linoleic (C18:2, $\geq 95\%$) acids by Alfa Aesar, palmitic (C16:0, $\geq 99\%$) acid by Sigma Aldrich, palmitoleic (C16:1, $\geq 99\%$) acid by Scbt, myristic (C14:0, $\geq 98\%$) acid by Scharlau. The quantitative analysis was performed in SIM modality, selecting three representative m/z peaks for each FA.

Results and discussion

Preparation and characterization of solid CoMo/ γ -Al₂O₃ catalysts

Two different approaches for the aqueous phase synthesis of mesoporous CoMo/ γ -Al₂O₃ catalysts are compared. In a first approach, called “impregnation”, a nanostructured γ -Al₂O₃ material is first prepared using the supramolecular assemblies formed between the randomly methylated β -cyclodextrin (RaMe β -CD) and the Pluronic F127 as soft template, and sol-gel boehmite (AlO(OH)) nanoparticles as building blocks. After thermal treatment at 500 °C, the porous support is impregnated with an aqueous solution of Co and Mo in presence of the native β -CD. Here, the RaMe β -CD acts as pore expander allowing for tailoring the pore size of γ -Al₂O₃,^{32,33} while the native β -CD acts as dispersing agent, providing uniform distribution of active elements over the porous support³⁴ (Figure 2 A). In a second approach, referred to as “one-pot”, Co and Mo are encapsulated directly into the supramolecular assemblies formed between the RaMe β -CD and a block copolymer (Pluronic F127 or Tetronic T90R4) around which boehmite colloids self-

assemble (Figure 2 B). Here, the metallo-supramolecular assemblies play a dual role; they increase the pore size and surface area of the alumina support and, simultaneously, promote uniform dispersion of metal oxide nanoparticles within the solid matrix. In both approaches, a thermal treatment is performed at 500 °C to remove the CD-based assemblies leaving behind Co and Mo oxide nanoparticles deposited onto the pores (impregnation method) or incorporated into the alumina framework (one-pot approach).

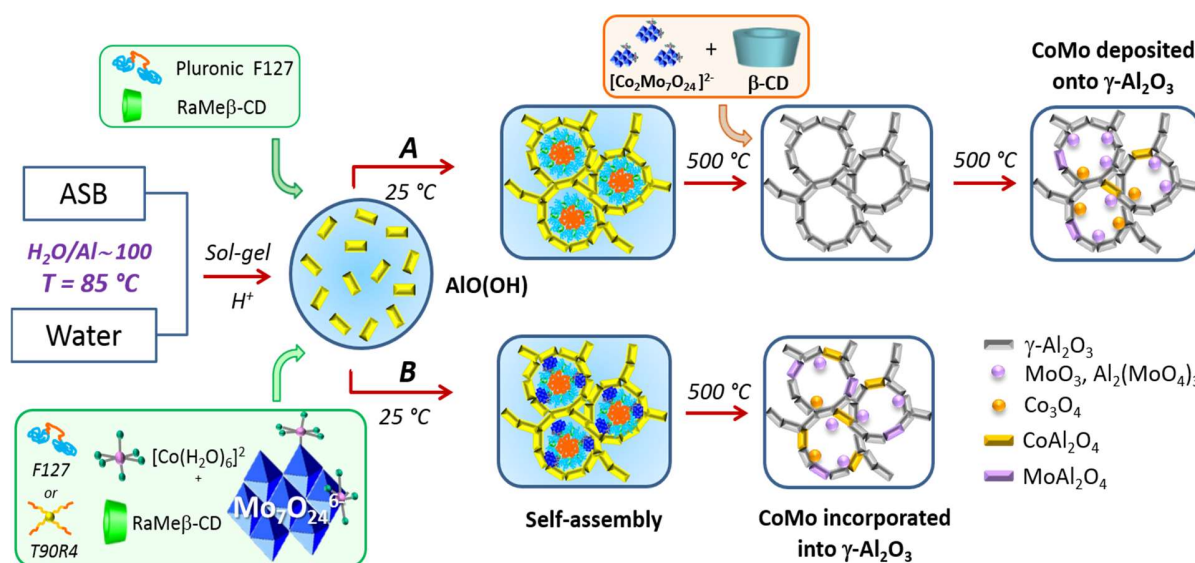


Figure 2. Schematic illustration for the preparation of γ - Al_2O_3 supported CoMo catalysts: A) two-steps impregnation using RaMe β -CD-F127 assemblies as template and native β -CD as dispersing agent and B) one-pot colloidal approach using the metallo-supramolecular assemblies as template.

Before preparing the supported catalysts, the interactions between metal salts and supramolecular assemblies were studied using UV-visible spectroscopy. The pH of all solutions was maintained fixed at 5.

Figure 3 A shows the UV-visible spectra recorded on mixtures prepared with 0.02 M Co (II) and increasing concentrations of Mo (VI), from 0.07 to 1.42 M. The Co (II) solution prepared without

Mo presents an intense absorption band at 511 nm with a shoulder at 473 nm corresponding to d-d transitions of the $[\text{Co}(\text{H}_2\text{O})_6]^{2+}$ complex,³⁵ while the Mo (VI) solution prepared without Co shows only one absorption below 400 nm, characteristic of the ligand-to-metal $\text{O}^{2-} \rightarrow \text{Mo}^{6+}$ charge transfer (LMCT). Upon addition of increasing amounts of Mo (VI) to the Co (II) solution, the d-d transition of the $[\text{Co}(\text{H}_2\text{O})_6]^{2+}$ complex progressively increases in intensity, while the onset of the $\text{O} \rightarrow \text{Mo}$ (VI) LMCT shifts to higher wavelengths. This is an indication that cobalt cations (Co^{2+}) interact with heptamolybdate anions ($\text{Mo}_7\text{O}_{24}^{6-}$) yielding bimetallic CoMo complexes. These results are in agreement with those reported by Weckhuysen *et al.*³⁵ who proposed on the basis of Raman and UV-vis-NIR spectroscopy a molecular structure for the CoMo complex, similar to that of Fe- and Mn-heptamolybdates³⁶ in which $\text{Co}(\text{II})$ cations are coordinated to $\text{Mo}_7\text{O}_{24}^{6-}$ anions *via* one or two oxygens, as shown in Figure 3 A (inset). Interestingly, pronounced changes in the band position and intensity of diluted CoMo solutions (4 mM Co and 56 mM Mo) were observed upon addition of RaMe β -CD-F127 and RaMe β -CD-T90R4 assemblies indicating changes in the electronic environment of the CoMo complex (Figure 3 B). Thus, the disappearance of the band at 516.5 nm coincides with the appearance of new absorption bands at 569.2 and 567.7 nm resulting from the formation of new metallo-supramolecular assemblies. These bands are somewhat flattened for CoMo-RaMe β -CD-F127 mixtures and rather intense for CoMo-T90R4 and CoMo-RaMe β -CD-T90R4 ones, consistent with the dark brown color of these latter. Such particular behavior of Tetronic-based assemblies may be explained by the establishment of electrostatic interactions between the negatively charged $[\text{Co}_2\text{Mo}_7\text{O}_{24}]^{2-}$ complex and the positively charged amino groups of the T90R4 block copolymer at pH 5. Indeed, the presence of two tertiary amine groups in the center of the poloxamine confers to this molecule a pH sensitive behavior.³⁷ The two pKa values of Tetronic T90R4 are reported to be 4.34 and 8.15, as determined

by potentiometric titration.³⁸ Thus, below pH 4.34, the ethylene diamine is diprotonated, while at pH values between 4.34 and 8.15, as is the case here, the monoprotinated form is predominant. In contrast to Pluronic, which does not contain any pH-sensitive moieties in its structure, the protonated amino groups in Tetronic must provide stronger metal-template interactions.

Remarkably, because of these interactions, the stability of metallo-supramolecular assemblies was greatly affected. Thus, visual inspection of two-months aged template-free CoMo solutions revealed formation of a suspension of solid particles which precipitated over time as a hydrated solid (Figure 4 A). Mixtures prepared with higher Mo loadings precipitated faster than those prepared with lower Mo loadings. Examination of the precipitate by X-ray diffraction revealed the formation of highly crystalline compounds ascribed to the monoclinic $(\text{NH}_4)_4(\text{Mo}_8\text{O}_{24.8})(\text{O}_2)_{1.2}(\text{H}_2\text{O})_2(\text{H}_2\text{O})_4$ (JCPDS card No 88-1326) and the triclinic $(\text{NH}_4)_2\text{Mo}_4\text{O}_{13}$ (JCPDS card No 80-0756) phases (Figure 4 B). In a marked contrast with the template-free CoMo solution, CoMo-RaMe β -CD-F127 and CoMo-RaMe β -CD-T90R4 mixtures were homogenous and stable for several months.

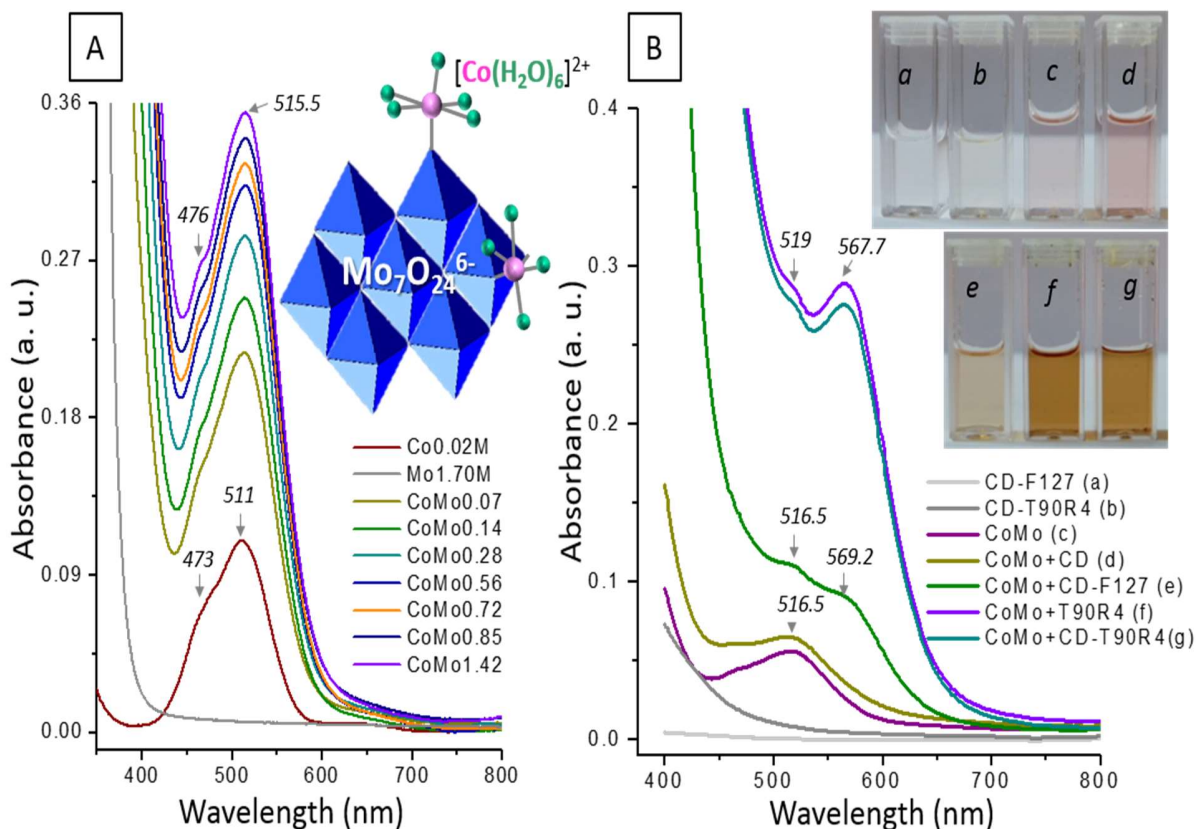


Figure 3. UV-vis spectra of: (A) CoMo aqueous solutions prepared with 0.02M Co and increasing concentrations of Mo (from 0.07 to 1.42 M); (B) CD-polymer assemblies (1.3% RaMe β -CD; 0.7%F127; 0.7%T90R4) prepared without and with CoMo (4mM Co and 56mM Mo). Inset photos: visual aspect of the different mixtures.

To gain further insight into the co-assembly behavior and stability of these metallo-supramolecular assemblies, Dynamic Light Scattering (DLS) measurements were performed on freshly prepared and two-months aged solutions (Figure 4 C, D). The intensity size distributions of CoMo-RaMe β -CD-F127 mixtures (4 mM Co and 56 mM Mo, 0.7% F127 and 1.3% RaMe β -CD) indicate that at 25 °C, the main scattering species are RaMe β -CD and Pluronic oligomers with an apparent hydrodynamic radius (R_H) of 1.5 and 5.3 nm respectively (Figure 4 C). Aging the

solutions at room temperature for two months has almost no impact on the aggregation behavior. Micelles start forming at 30 °C with an R_H of 22.3 nm, while a small amount of residual non-assembled species still exists in solution ($R_H = 2.4$ nm). Between 30 and 50 °C, micelles remain stable, although a slight shift of the intensity distribution towards lower sizes (from 24 to 18 nm) is observed due to dehydration of the hydrophobic core.³⁹ No phase separation occurs in this temperature range. On the other hand, for CoMo-RaMe β -CD-T90R4 assemblies (4 mM Co and 56 mM Mo, 0.7%T90R4 and 1.3% RaMe β -CD), unimers are the only scattering species at 25 °C with an apparent hydrodynamic radius of 2.2 nm, consistent with the value reported in literature for T90R4 (Figure 4 D).³⁸ Aging the solutions at room temperature for two months and increasing the temperature to 30 °C provokes a broadening of size distributions, indicating the beginning of the agglomeration process. At 40 °C, micelles are the main scattering species ($R_H = 6.2$ nm), while at higher temperatures the solution becomes turbid and R_H abruptly shifts to higher sizes indicating the beginning of phase separation, in agreement with SANS and DSC data reported by Plestil *et al.*⁴⁰

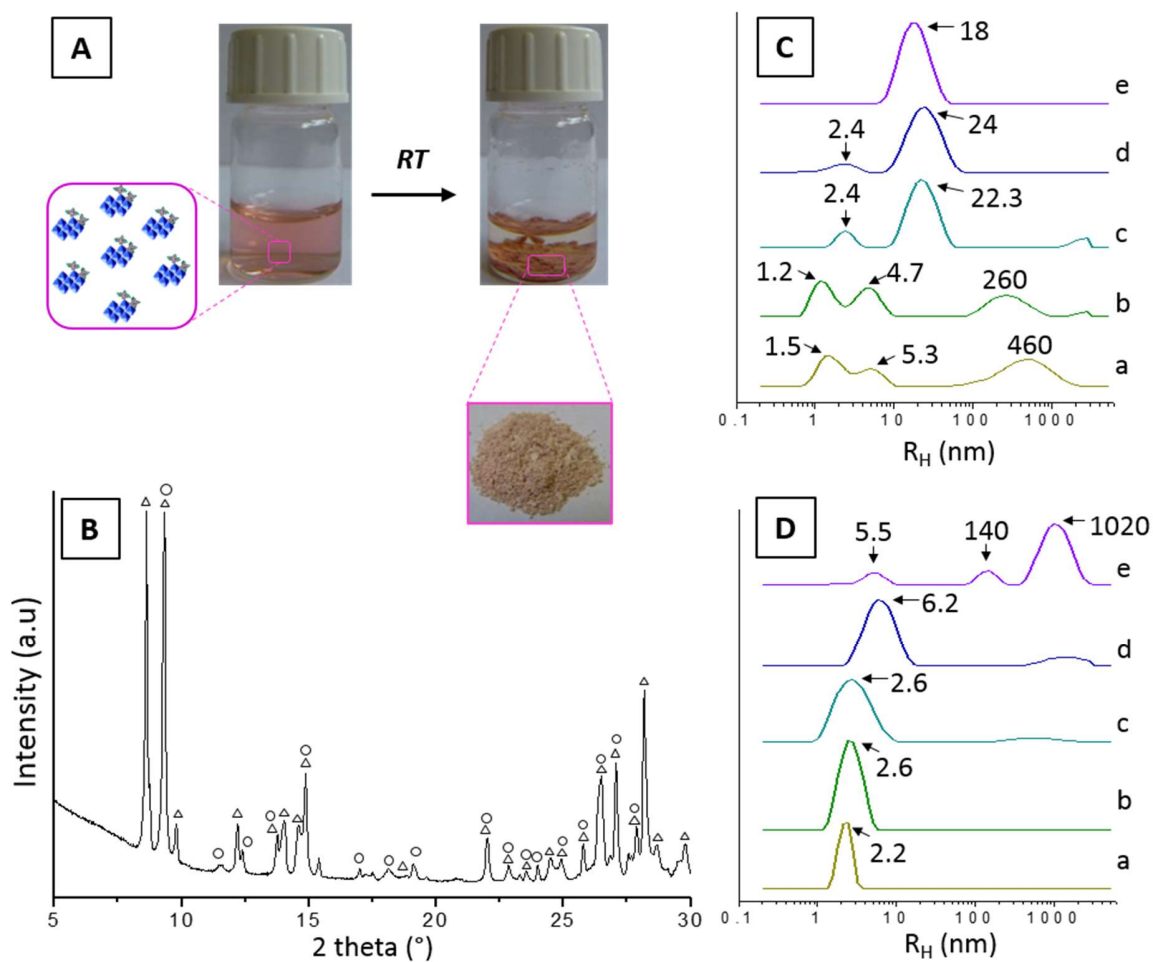


Figure 4. (A) Visual aspect of template-free CoMo solution (25 mM Co and 335 mM Mo) before and after aging for two months at room temperature (RT), (B) XRD diagram of the precipitated solid: (Δ) $(\text{NH}_4)_4(\text{Mo}_8\text{O}_{24.8})(\text{O}_2)_{1.2}(\text{H}_2\text{O})_2(\text{H}_2\text{O})_4$ and (\circ) $(\text{NH}_4)_2\text{Mo}_4\text{O}_{13}$; (C) DLS profiles of RaMe β -CD-F127-based metallo-supramolecular assemblies (4 mM Co, 56 mM Mo, 0.7% F127, 1.3% RaMe β -CD), and (D) DLS profiles of RaMe β -CD-T90R4-based assemblies (4 mM Co, 56 mM Mo, 0.7% T90R4, 1.3% RaMe β -CD). Fresh CoMo-template solutions (a) and two-months aged solutions at 25 $^\circ\text{C}$ (b); 30 $^\circ\text{C}$ (c); 40 $^\circ\text{C}$ (d) and 50 $^\circ\text{C}$ (e).

Taken together, these results evidence that specific interactions exist in aqueous solution between the $[\text{Co}_2\text{Mo}_7\text{O}_{24}]^{2-}$ complex and the supramolecular template, avoiding irreversible precipitation and yielding stable metallo-supramolecular assemblies. Such interactions are expected to impact the dispersion of Co and Mo oxide nanoparticles over the alumina support and this must have direct consequence on the stability and catalytic activity of $\text{CoMo}/\gamma\text{-Al}_2\text{O}_3$ materials.

To assess the validity of this statement, six $\text{CoMo}/\gamma\text{-Al}_2\text{O}_3$ catalysts were prepared using the two-steps impregnation method and the one-pot colloidal approach. Details about the preparation methods and the composition of each catalyst are given in Table 1.

Table 1. Mesoporous $\text{CoMo}/\gamma\text{-Al}_2\text{O}_3$ catalysts prepared by two different methods.

Catalyst	Preparation method	Introduction of $\text{Co}(\text{NO}_3)_2 \cdot 6\text{H}_2\text{O}$ and $(\text{NH}_4)_6\text{Mo}_7\text{O}_{24} \cdot 4\text{H}_2\text{O}$	Co (wt%)	Mo (wt%)
CoMo1		Only one impregnation of $\text{Mo}/\gamma\text{-Al}_2\text{O}_3^{\text{a}}$ with $\text{Co}+\beta\text{CD}$	0.6	6.4
CoMo2	Impregnation method	Two successive impregnations of $\gamma\text{-Al}_2\text{O}_3^{\text{b}}$: first $\text{Mo}+\beta\text{CD}$, then $\text{Co}+\beta\text{CD}$	0.6	6.4
CoMo3		Two successive impregnations of $\gamma\text{-Al}_2\text{O}_3$: first $\text{Mo}+\beta\text{CD}$, then $\text{Co}+\beta\text{CD}$	1.2	15.7
CoMo4		Simultaneous introduction of Co and Mo in $\text{RaMe}\beta\text{CD-F127-AlO}(\text{OH})$ assemblies	0.6	6.4
CoMo5	One-pot colloidal approach	Simultaneous introduction of Co and Mo in $\text{RaMe}\beta\text{CD-F127-AlO}(\text{OH})$ assemblies	1.2	15.7
CoMo6		Simultaneous introduction of Co and Mo in $\text{RaMe}\beta\text{CD-T90R4-AlO}(\text{OH})$ assemblies	1.2	15.7

^a $\text{Mo}/\gamma\text{-Al}_2\text{O}_3$ has been prepared by incorporating Mo into the $\text{RaMe}\beta\text{-CD-F127-AlO}(\text{OH})$ assemblies followed by drying and calcination at 500°C . ^bNanostructured $\gamma\text{-Al}_2\text{O}_3$ has been prepared using the $\text{RaMe}\beta\text{-CD-F127}$ assemblies as soft template and sol-gel $\text{AlO}(\text{OH})$ nanoparticles as building blocks. The material has been calcined at 500°C .

Figure 5 shows the Diffuse Reflectance (DR) UV-visible spectra of the catalysts prepared by impregnation (A, B) and colloidal approach (C, D). For all catalysts, the ligand-to-metal charge transfer (LMCT) $O^{2-} \rightarrow Mo^{6+}$ band can be observed in the 200-320 nm region (Figure 5 A, C). This band is comprised of two main peaks at 220-240 nm and 260-320 nm belonging to tetrahedron coordination Mo(Td) and low polymeric octahedral coordination Mo(Oh) species respectively.^{41,42} For the same CoMo loading (0.6% Co and 6.4% Mo), the absorption band of Mo(Td) species is better-defined for the one-pot catalyst (CoMo4) compared to impregnated ones (CoMo1 and CoMo2). This suggests that at low CoMo concentrations, RaMe β -CD-F127 assemblies promote formation of tetrahedral molybdenum species at the expense of octahedral ones, similarly to what has been observed previously with beta-FDU12/ γ -Al₂O₃ composites upon addition of EDTA.^{43,44} Note that the way of introduction of Co and Mo does not affect the spectral profiles which indicate very similar proportion of Mo(Td) and Mo(Oh) (see CoMo1 vs. CoMo2). On the other hand, the proportion of octahedral coordinated polymolybdate species increases with increasing the loadings in active elements (see CoMo3, CoMo5 and CoMo6).

More important differences on the spectral profiles were observed in the visible range (Figure 5 B, D). Thus, the three successive bands noticed at 540, 580 and 627 nm for all catalysts are ascribed to tetrahedron coordinated divalent Co species incorporated into the alumina framework as cobalt aluminate ($^4A_2(F) \rightarrow ^4T_1(P)$ transition, CoAl₂O₄, spinel).⁴⁵ Interestingly, for the same loading in active elements (0.6% Co and 6.4% Mo), these bands were better defined for the catalyst prepared by the one-pot approach (CoMo4) compared to those prepared by impregnation (CoMo1 and CoMo2). Moreover, further increase in the intensity of these bands was observed for higher loadings in active elements (1.2% Co and 15.7% Mo). Accordingly, this means that the one-pot colloidal approach facilitates the diffusion of Co²⁺ ions into the tetrahedral sites of γ -Al₂O₃ lattice,

thus promoting the formation of spinel cobalt aluminate. Actually, this triple band corresponds to a Jahn-Teller distortion of the tetrahedral structure which is also responsible for the blue coloration of CoAl_2O_4 , also known as Thenard's blue.⁴⁶⁻⁴⁹

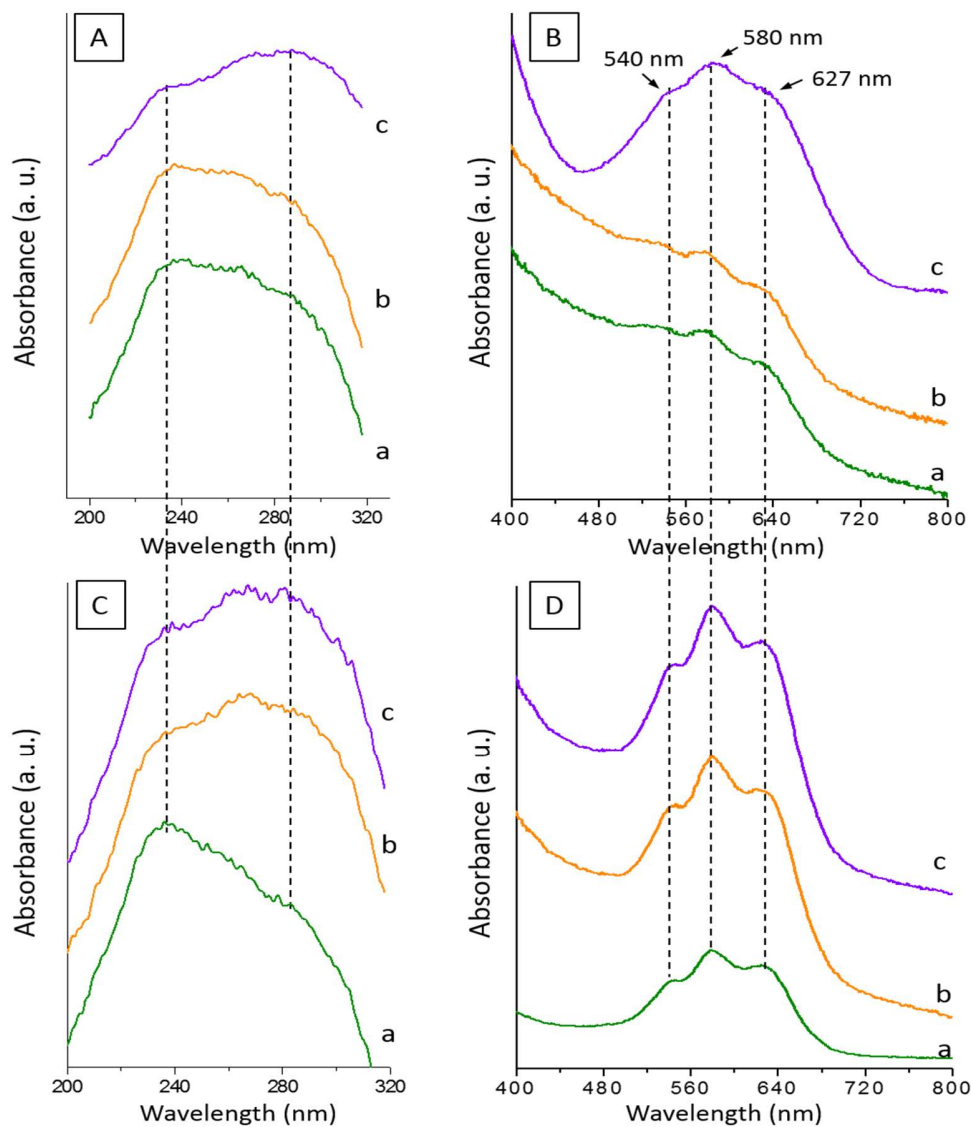


Figure 5. UV-vis diffuse reflectance spectra of $\text{CoMo}/\gamma\text{-Al}_2\text{O}_3$ catalysts prepared by impregnation (A, B): CoMo1 (a), CoMo2 (b), CoMo3 (c) and one-pot synthesis (C, D): CoMo4 (a), CoMo5 (b) and CoMo6 (c).

The X-ray diffraction patterns of all CoMo/ γ -Al₂O₃ catalysts present three broad peaks at 18.9°, 60.6° and 66.6° (Figure 6) attributed to the (111), (511) and (440) planes respectively of the γ -Al₂O₃ support (JCPDS card No 10-0425).

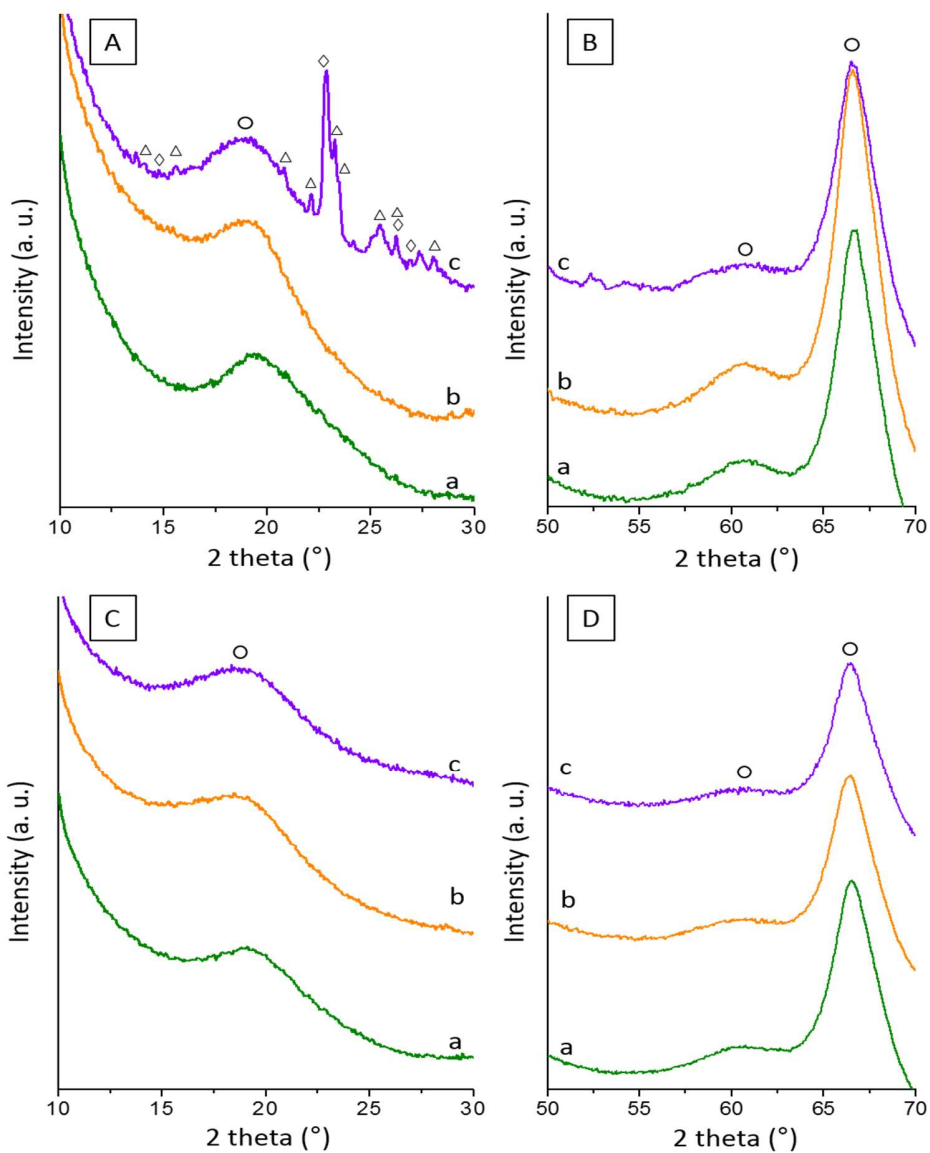


Figure 6. XRD patterns of CoMo/ γ -Al₂O₃ catalysts prepared by impregnation (A, B): CoMo1 (a), CoMo2 (b), CoMo3 (c) and one-pot synthesis (C, D): CoMo4 (a), CoMo5 (b) and CoMo6 (c). (○) γ -Al₂O₃, (Δ) Al₂(MoO₄)₃, (◇) MoO₃.

Except for CoMo₃, no other obvious signals could be observed for the other catalysts. This means that Co and Mo oxide particles may be either amorphous or composed of very small crystallites. Conversely, from the XRD pattern of CoMo₃, it can be seen that in addition to the diffraction peaks of MoO₃ phase (JCPDS card No 09-0209), other strong signals appear corresponding to the Al₂(MoO₄)₃ phase (JCPDS card No 84-1652). This is an indication that surface MoO₃ nanoclusters interact with γ -Al₂O₃ support and transform into Al₂(MoO₄)₃ which is a stable thermodynamic phase formed during the thermal treatment. Note that for all catalysts, the diffraction peaks of crystalline Co₃O₄ or CoO are not observed in the XRD patterns, indicating that these oxides do not form on the γ -Al₂O₃ surface.^{50,51} Instead, they tend to transform into CoAl₂O₄, in agreement with UV-vis data. Nevertheless, from the XRD patterns, it is difficult to distinguish CoAl₂O₄ from γ -Al₂O₃ because these two phases crystallize both in a cubic spinel structure and have very similar lattice parameters.⁵²

The reducibility behavior of these materials was investigated using H₂-temperature programmed reduction (H₂-TPR) measurements (Figure 7). For all catalysts, the peaks at 335 and 600 °C, characteristics of the reduction of cobalt oxides (Co₃O₄ and CoO respectively)⁵³ were not observed in TPR profiles, in agreement with XRD data. The catalysts prepared by impregnation present three peaks ascribed to the reduction of Co and Mo species in a three steps process: first, the partial reduction of amorphous, highly defective, multi-layered oxides octahedral Mo⁶⁺ species (peak at 540-560 °C),^{54,55,56} then the reduction of surface Al₂(MoO₄)₃^{57,58} and MoO₃ crystallites (peaks at *c.a.* 670-690 °C),^{50,55,56} and finally the deep reduction of all Co and Mo species incorporated into the alumina framework, including the highly dispersed tetrahedral (monomer) Mo⁴⁺ oxo-species^{50,54,55} and more stable CoAl₂O₄ and MoAl₂O₄ species (peaks at 940-960 °C) in strong interaction with the support. By contrast, the catalysts prepared by one-pot colloidal approach

present only two peaks at 540-560 °C and 940-960 °C indicating that the reduction of Co and Mo species is now performed in a two-steps process. The absence of additional reduction peaks at 670-690 °C suggests stronger interactions between the active elements and the γ -Al₂O₃ surface, thus hindering the formation of MoO₃ and Al₂(MoO₄)₃ crystallites on the support surface.^{50,59} Note that among the catalyst prepared by one-pot approach, CoMo6 displays the highest Mo⁶⁺ reduction temperature (562 °C) resulting from stronger metal-support interactions.

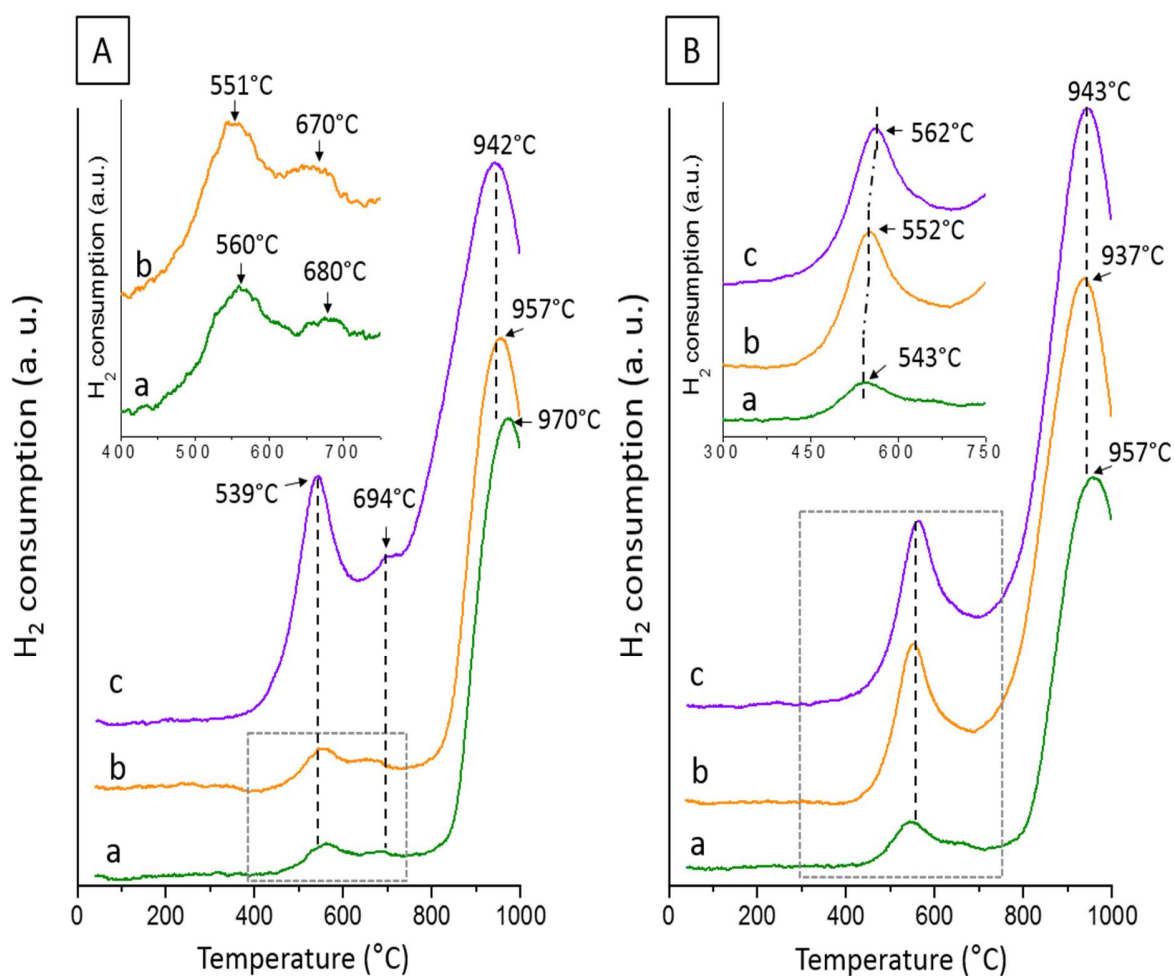


Figure 7. H₂-TPR profiles of CoMo/ γ -Al₂O₃ catalysts prepared by impregnation (A): CoMo1 (a), CoMo2 (b), CoMo3 (c) and one-pot approach (B): CoMo4 (a), CoMo5 (b) and CoMo6 (c).

The impact of the metallo-supramolecular assemblies on the textural characteristics of the catalysts was evaluated by N₂-adsorption analysis. Figure 8 depicts the adsorption isotherms and corresponding pore size distributions (inset) for the catalysts prepared by impregnation (Figure 8 A) and one-pot approach (Figure 8 B).

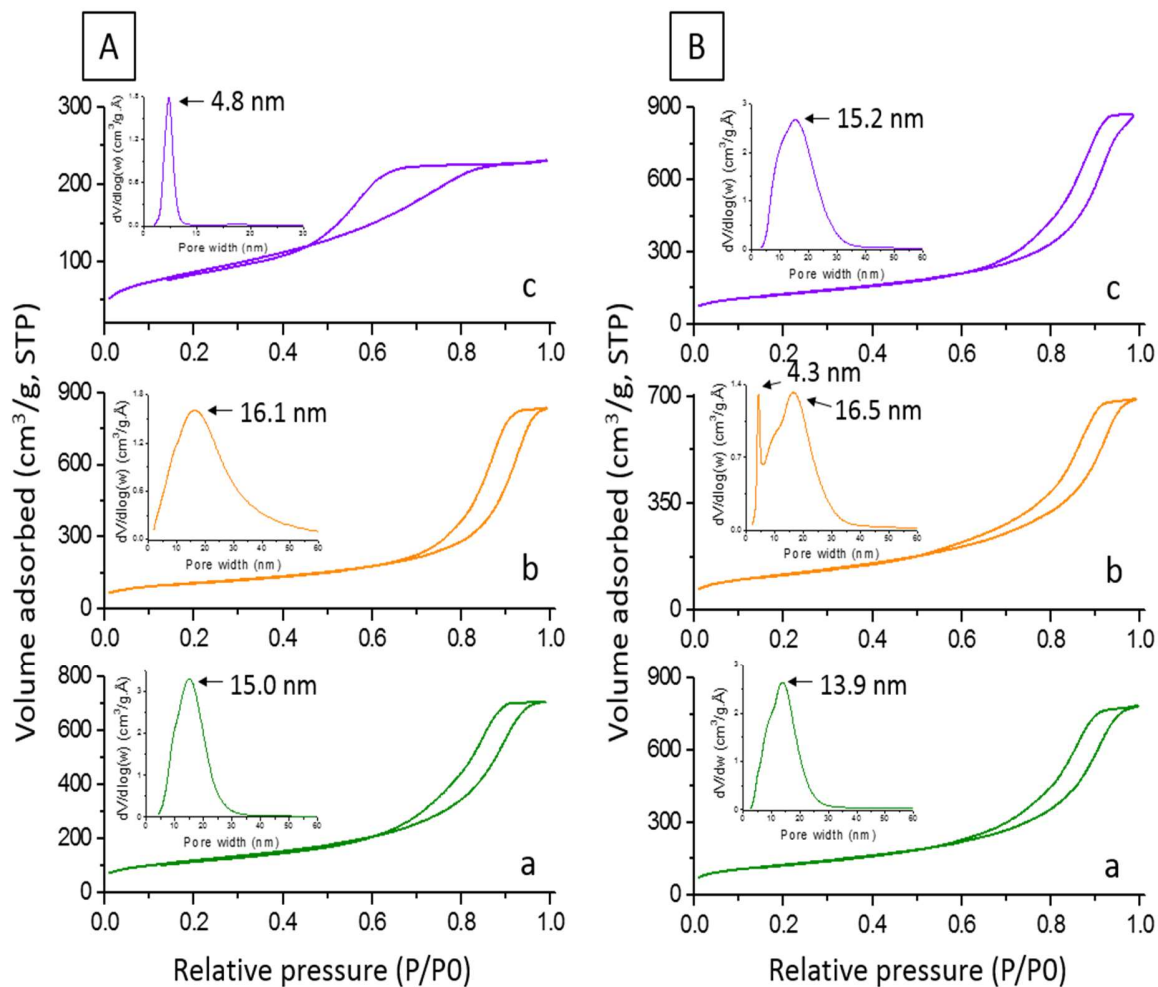


Figure 8. Evolution of the adsorption-isotherms and pore size distributions (inset) for CoMo/ γ -Al₂O₃ catalysts prepared by impregnation (A): CoMo1 (a), CoMo2 (b), CoMo3 (c) and one-pot approach (B): CoMo4 (a), CoMo5 (b) and CoMo6 (c).

All catalysts display type-IV isotherms which are characteristic of mesoporous materials. Note that the highest specific surface areas (410-440 m² g⁻¹) are obtained for the catalysts prepared by one-pot approach (Table 2). Moreover, whatever the preparation method, for low CoMo loadings (0.6% Co and 6.4% Mo), the pore size is not significantly altered compared to the support alone (γ -Al₂O₃ prepared without CoMo has a pore diameter of 15.5 nm). This means that the active elements are either dispersed as small particles or incorporated into the walls of alumina. On the other hand, for higher loadings in active elements (1.2% Co and 15.7% Mo), the pore size of the impregnated catalyst (CoMo3) abruptly decreases to 4.8 nm as a result of the filling of pores. Conversely, the pore size of the one-pot catalysts (CoMo5 and CoMo6) prepared with the same loadings remains almost unchanged, indicating the presence of open pores > 11 nm.

Table 2. Textural characteristics of CoMo/ γ -Al₂O₃ catalysts after thermal treatment at 500 °C.

Sample	Co(wt%)	Mo(wt%)	S _{BET} ^a (m ² g ⁻¹)	PV ^b (cm ³ g ⁻¹)	PS ^c (nm)
<i>Impregnation method</i>					
CoMo1	0.6	6.4	418	1.10	15.0
CoMo2	0.6	6.4	373	1.29	16.1
CoMo3	1.2	15.7	306	0.35	4.8
<i>One-pot colloidal approach</i>					
CoMo4	0.6	6.4	437	1.17	13.9
CoMo5	1.2	15.7	411	1.08	4.3 and 16.5
CoMo6	1.2	15.7	429	1.36	15.2

^aBET specific surface area determined in the relative pressure range 0.1-0.25, ^bPV = cumulative pore volume (BJH), ^cPS = pore size calculated from BJH method.

Hydrothermal stability of supported catalysts

It is well-known that γ -Al₂O₃ is thermodynamically unstable under harsh hydrothermal conditions.⁶⁰ At 150 °C or above, γ -Al₂O₃ transforms into hydrated boehmite (AlO(OH)) which is more stable than both gibbsite (Al(OH)₃) and γ -Al₂O₃ in hot water. This transformation usually results in a drastic reduction of surface area of the material⁶¹ and complete loss of Lewis acidity,²¹ which in turn provokes sintering of metal nanoparticles deposited on the support surface.^{21, 62, 63}

The supported catalysts were exposed under the same operative hydrothermal conditions adopted to perform the liquefaction of microalgae (375 °C for 15 minutes under autogenic pressure). All catalysts underwent changes in their crystalline structure due to partial or total rehydration of the γ -Al₂O₃ surface and transformation to its hydrated form, boehmite, as deducible from XRD characterization (Figure 9).

Thus, for CoMo1 and CoMo2 catalysts, only the sharp reflexions of AlO(OH) (JCPDS card No 21-1307) are observed indicating total alumina-to-boehmite phase transformation, while a higher resistance to rehydration is noticed for all one-pot catalysts. Moreover, in the case of CoMo3, although the major diffraction peaks of Al₂(MoO₄)₃ disappeared, the stability of γ -Al₂O₃ support was not much affected by the hydrothermal conditions.

It has been established by both adsorption micro-calorimetry experiments and thermodynamic calculations, combined with DFT models,⁶⁴ that γ -Al₂O₃ easily transforms in hot water into hydrated boehmite due to the negative free energy of this reaction. Indeed, the free energy of transformation of pure γ -Al₂O₃ to boehmite has been calculated to be -42.8 kJ mol⁻¹ with H₂O (gas) and -34.3 kJ mol⁻¹ with H₂O (liquid) which makes this transformation thermodynamically favorable.⁶⁵ Under hydrothermal conditions, it is therefore difficult to obtain exactly the same structure as the fresh catalyst because of the energetic instability of bare γ -Al₂O₃. Nevertheless,

the transformation kinetics can be considerably slowed down by introducing doping elements. For instance, the adsorption micro-calorimetry experiments as a function of hydroxyl coverage have shown that the adsorption enthalpy of Zr-doped γ -Al₂O₃ is less negative than that of bare γ -Al₂O₃ (-130 kJ mol⁻¹ vs. -38 kJ mol⁻¹ for 5 OH nm⁻² coverage), while no significant change was observed in the presence of Mg (-110 kJ mol⁻¹ for 5 OH nm⁻² coverage).⁶⁶ Moreover, the enthalpies of alumina-to-boehmite transformation became less exothermic with increasing the dopant loading, indicating a lowering of the surface energy of γ -Al₂O₃ by the zirconium additive.

In agreement with these studies, our results show that when cobalt and molybdenum are used as dopants, the hydrothermal stability of γ -Al₂O₃ can be significantly enhanced. More importantly, the way how Co and Mo are introduced into the γ -Al₂O₃ framework appears to have a strong impact on the catalyst stability. Thus, for low metal loadings, the XRD data indicate that while the catalysts prepared by impregnation are totally transformed into boehmite, the catalysts prepared by the one-pot approach exhibit only marginal changes in their crystalline structure indicating a high resistance against hydrolysis.

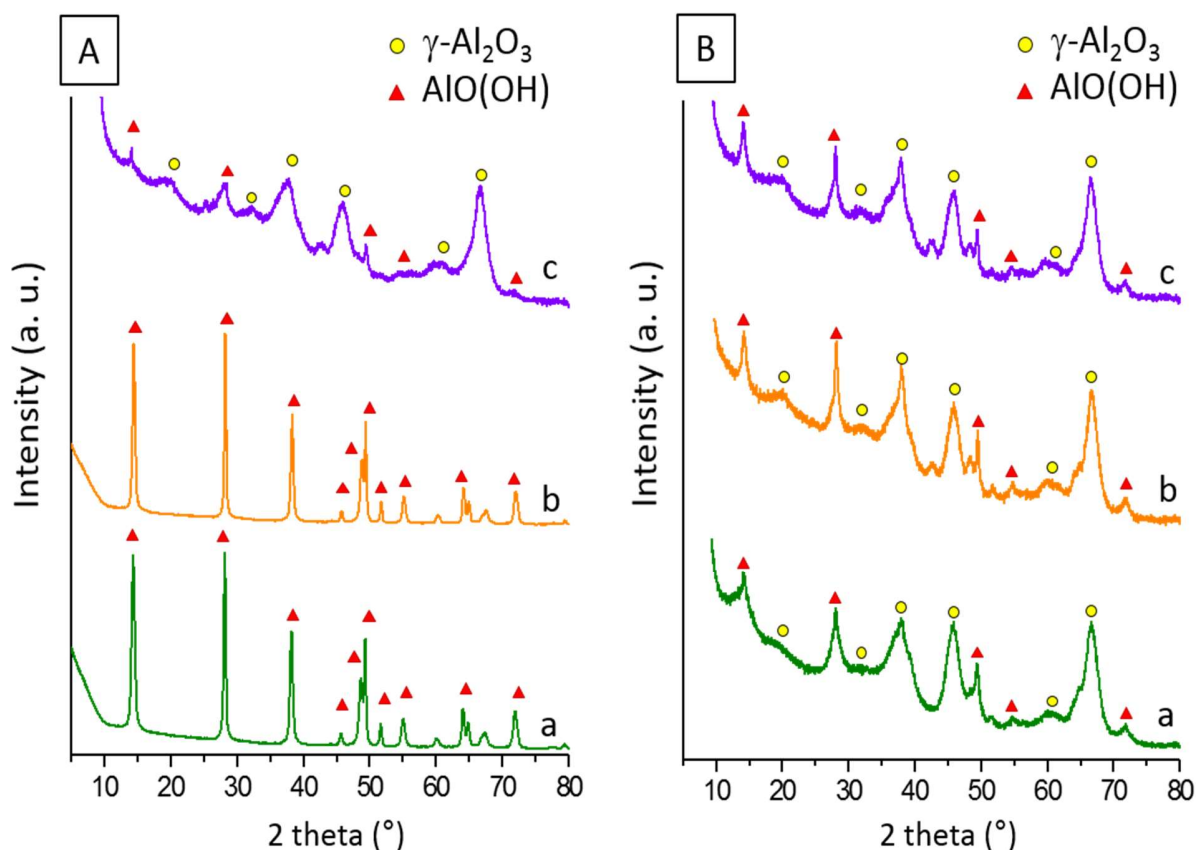


Figure 9. XRD patterns of CoMo/ γ -Al₂O₃ catalysts prepared by impregnation (A): CoMo1 (a), CoMo2 (b), CoMo3 (c) and one-pot approach (B): CoMo4 (a), CoMo5 (b) and CoMo6 (c) after exposure in hydrothermal environment at 375 °C for 15 minutes.

Further evidence for such difference in the hydrothermal stability was provided by N₂-adsorption analysis. The adsorption isotherms and pore size distributions are compared in Figure 10. Clearly, the isotherms present different shapes depending on the catalyst loading and the preparation method. CoMo1 and CoMo2 show a type IV isotherm with a type H3 hysteresis loop characteristics of materials with large slit-shape mesopores and macropores.⁶⁷ The pore size distribution dramatically broadens compared to non-treated catalysts (Figure 8) and shifts to higher sizes indicating a structural collapse. Consequently, the specific surface area drops from 360-370

to 20-50 m²/g, representing an average loss of 86-96 % relative to the initial value (Table 3). Conversely, all one-pot catalysts present a type H1 hysteresis loop with a well-defined plateau at high relative pressures and a narrow pore size distribution indicating that the mesoscopic order is now preserved. The reduction of pore sizes from 11-13 to 4-6 nm points however towards a densification of the catalyst network. Moreover, the loss in surface areas is much slower than for impregnated catalysts (S_{BET} drops from 410-440 to 280-290 m²/g representing an average loss of 33-35%). This is an indication that the one-pot catalysts prepared with low CoMo loadings undergo slower deactivation compared to the impregnated catalysts prepared with the same CoMo loadings. Most probably, cobalt- and molybdenum-aluminates, which make-up the majority of the former catalysts, are able to create a physical barrier towards water, thus opposing alumina-to-boehmite phase transformation. On the other hand, for CoMo₃ prepared with high CoMo loadings, the loss in surface area was found to be less severe (only 7%) compared to the analogous one-pot catalysts (CoMo₅ and CoMo₆). Similar stabilizing effect against transformation of γ -Al₂O₃ to boehmite in hot liquid water was recently observed in the presence of biomass-derived compounds, such as two- or three-carbon polyols, as well as lignin, which showed the ability to adsorb over γ -Al₂O₃ support²² or Pt/ γ -Al₂O₃ catalysts.^{20,23} Indeed, the multidentate interactions established between lignin and γ -Al₂O₃ *via* the oxygen functionalities were shown to prevent formation of boehmite phase and sintering of the supported Pt nanoparticles.²³

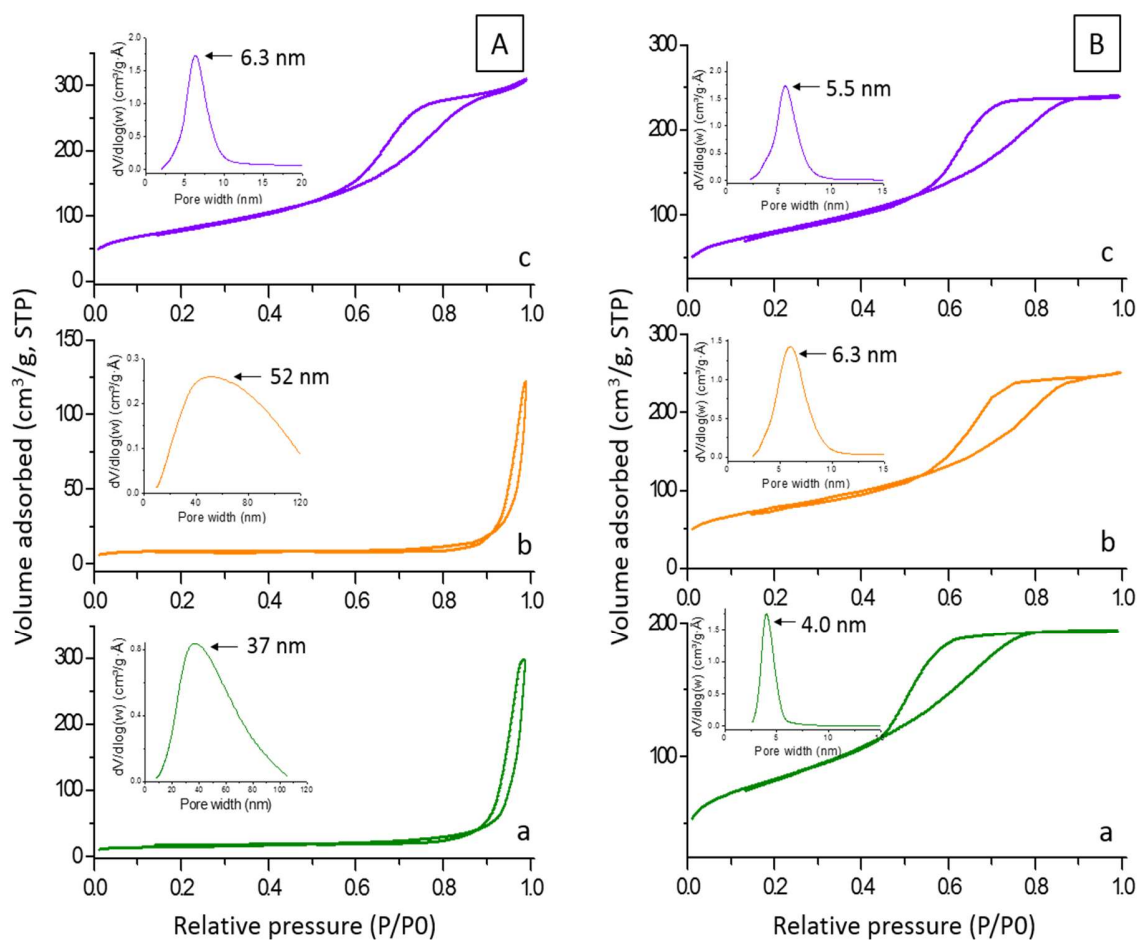


Figure 10. N₂-adsorption isotherms and corresponding pore size distributions (inset) of CoMo/ γ -Al₂O₃ catalysts prepared by impregnation (A): CoMo1 (a), CoMo2 (b), CoMo3 (c) and one-pot approach (B): CoMo4 (a), CoMo5 (b) and CoMo6 (c) after exposure in hydrothermal environment at 375 °C for 15 minutes.

Based on the above results, the proposed mechanism through which metal oxide nanoparticles are supposed to interact with the nanostructured γ -Al₂O₃ support prepared from RaMe β -CD-based assemblies is illustrated in Figure 11. When cobalt and molybdenum species are dispersed at low concentration over the γ -Al₂O₃ support by impregnation, small and well-dispersed metal oxide nanoparticles form on the support surface without affecting significantly its structural and textural

properties but, with a failure to stabilize the support against hydrolysis in hot water. Increasing the metal loading promotes partial diffusion of metal oxide nanoparticles into the walls of alumina, and leads to formation of surface $\text{Al}_2(\text{MoO}_4)_3$ and MoO_3 crystallites. High Co and Mo loadings are necessary to ensure diffusion of these species into the alumina framework and stabilize the material under hydrothermal conditions.

On the other hand, the incorporation of $[\text{Co}_2\text{Mo}_7\text{O}_{24}]^{2-}$ complex directly within the supramolecular template promotes diffusion of the active elements into the walls of $\gamma\text{-Al}_2\text{O}_3$, even at low CoMo loadings, thus leading to small and well-dispersed metal oxide nanoparticles and hydrothermally stable catalysts. Such diffusion of Co and Mo into the pores of the support occurs during the crystallographic conversion of boehmite into $\gamma\text{-Al}_2\text{O}_3$ at 500 °C.

Table 3. Textural characteristics of mesoporous $\text{CoMo}/\gamma\text{-Al}_2\text{O}_3$ catalysts after exposure in hydrothermal environment at 375°C for 15 minutes.

Sample	$S_{\text{BET}}^{\text{a}}$ ($\text{m}^2 \text{g}^{-1}$)	PV^{b} ($\text{cm}^3 \text{g}^{-1}$)	PS ^c (nm)	S_{BET} loss (%)
<i>Impregnation method</i>				
CoMo1-375	51	0.47	37	88
CoMo2-375	30	0.20	52	92
CoMo3-375	286	0.49	6.3	7
<i>One-pot colloidal approach</i>				
CoMo4-375	293	0.28	4.0	27
CoMo5-375	275	0.39	6.3	33
CoMo6-375	287	0.36	5.5	33

^aBET specific surface area determined in the relative pressure range 0.1-0.25, ^bPV = cumulative pore volume (BJH), ^cPS = pore size calculated from BJH method.

The crystalline structure of boehmite is planar and built-up of oriented sheets of octahedral (Oh) aluminum units connected *via* hydrogen bonds,⁶⁸ while the crystalline lattice of γ -Al₂O₃ is cubic spinel and built-up of close-packed stacked oxygen layers where Al³⁺ ions occupy both the octahedral (Oh) and the tetrahedral (Td) sites and where some lattice sites remain empty in order to satisfy the stoichiometry of γ -Al₂O₃. The thermal transformation of nanocrystalline boehmite into γ -Al₂O₃ has previously been modelled by a four steps reaction mechanism^{69,70} involving (i) the removal of physisorbed water located in the interlayer space, (ii) the removal of chemisorbed water, (iii) the structural collapse of boehmite, and (iv) the transfer of first aluminum species from octahedral to tetrahedral sites. Surface hydroxyl groups have been shown to condensate first, followed by bulk hydroxyls, before complete transformation to γ -Al₂O₃ with an equilibrium structure containing about 25-31% of tetrahedral aluminum sites.⁶⁹

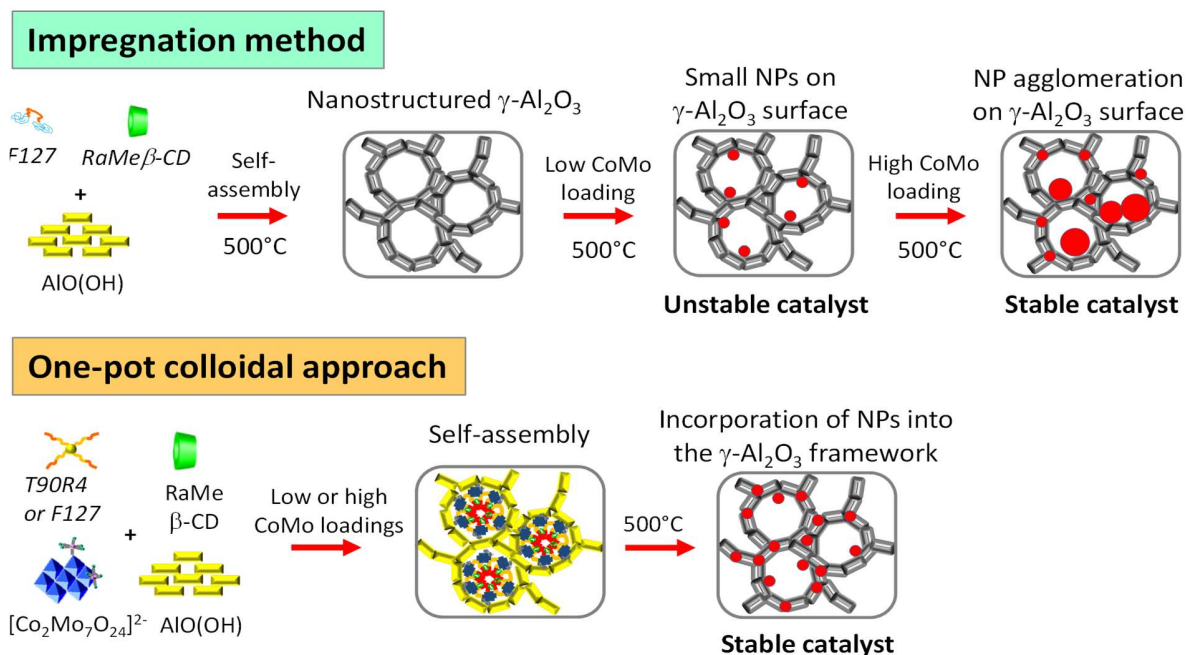


Figure 11. Proposed formation mechanism of mesoporous CoMo/ γ -Al₂O₃ catalysts prepared *via* impregnation and template-assisted one-pot colloidal approach.

A DFT study⁷¹ has shown that the basal (010) faces of AlO(OH), which have the lowest interfacial tension, tend to attain the highest development. This explains the low thickness of AlO(OH) nanoparticles (~ 3 nm) and the fiber-like structure of the resulting γ -Al₂O₃ material.⁷² When the supramolecular assemblies formed between the block copolymer and the RaMe β -CD are introduced into the boehmite sol, they interact weakly, through hydrogen bonding, with the basal surface hydroxyl groups.³² Moreover, as cobalt and molybdenum species are encapsulated directly into these assemblies, the template removal during calcination at 500 °C should facilitate incorporation of these ions into the Td and Oh sites of the cubic spinel structure. Consequently, in addition to their important role in enhancing the porosity and surface area of the support, the supramolecular assemblies may also facilitate incorporation of cobalt and molybdenum within the alumina framework during the crystallographic conversion of boehmite, thus resulting in stabilization against hydrolysis.

Cobalt ions, with lower cationic charge, should diffuse preferentially into the tetrahedral sites. Indeed, the presence of the triple absorption band in the 540-630 nm region (Figure 5 B, D), as well as the blue color of these catalysts, are typical of Co²⁺ in a tetrahedral environment. Actually, the formation of cobalt aluminates results from the lattice matching between γ -Al₂O₃ and CoAl₂O₄,⁷³ both of which adopt a cubic spinel structure with the same space group (Fd3m) and have very similar lattice constant values (*i.e.* 7.9 Å for γ -Al₂O₃⁷⁴ and 8.1 Å for CoAl₂O₄⁵²). On the other hand, molybdenum ions, with higher cationic charge, are forced to enter preferentially into the octahedral sites, although a small portion of tetrahedral molybdenum species is also detected in the UV spectra (Figure 5 A, C). The proportion of tetrahedral and octahedral coordinated polymolybdate species appears, however, to be dependent on the concentration in active elements; the octahedral environment being favored for the highest Mo loadings. Notably, CoMo₃ prepared

with the highest metal loadings, displayed only marginal loss in surface area and negligible hydrolysis to boehmite. Such a particular behavior of this catalyst may be explained by the distribution of the active elements between the interior and the exterior surface of the porous support, thus hindering the interactions of water molecules with both the surface and bulk hydroxyl groups of alumina, thus preserving the support from hydrolysis.

Previous studies have shown that cobalt aluminates can be highly active toward the oxidation of CO⁷⁵ and the decomposition of H₂O₂ at room temperature.⁷³ However, to our knowledge, no detailed investigation of the structure-property relationships in supported bimetallic CoMo/ γ -Al₂O₃ catalysts for the liquefaction of microalgae has been performed to date. As reported in many articles, the structural and textural characteristics of the heterogeneous catalysts, as well as the distribution of the active elements, may have a great impact on both the diffusion of the reactants and the products yields.^{76,77,78} In what follows, we discuss how the preparation method may affect the catalytic performances of mesoporous CoMo/ γ -Al₂O₃ catalysts in the hydrothermal liquefaction of microalgae.

Catalytic performances

The six prepared catalysts were tested in the hydrothermal liquefaction of microalga *Nannochloropsis gaditana* whose proximate and ultimate analyses are reported in Table 4. HTL tests were performed at 375 °C. The reaction time was fixed at 15 min in order to limit loss of biocrude due to follow-up reactions, such as cracking and repolymerization, which would otherwise enhance gas and char formation.⁷⁹ Thus, as pointed out by Alba *et al.*⁸⁰, when working near the critical point of water (*i.e.* 374°C), short reaction times appear to be more convenient for a maximum oil production. The reactor was unstirred that is a frequent choice to study the effect

of catalysts in the HTL of microalgae in batch reactors. This means that bio-constituents of the solid biomass, *i.e.* proteins, polysaccharides, triglycerides, are first hydrolyzed by hot water. The heterogeneous catalyst will work on the products of aforementioned decomposition reactions dissolved in the fluid phase. It must be considered that reactions were performed at near critical conditions in which small temperature gradient can activate significant natural convection inside the reactor. For this reason, even if the reactor was not stirred, mass transfer was not only diffusional but also promoted by convection.⁸¹ The results of HTL tests performed with the six catalysts are reported in Figure 12 together with the results of an experiment without added catalyst.

Table 4. Proximate and ultimate analyses of the *Nannochloropsis gaditana* microalga adopted for HTL tests; the composition values are weight percentages referred to the dry microalga mass.

Proteins			Lipids		Carbohydrates			Ashes
38.0			24.1		10.7			27.2
C	H	N	S	O ^a	H/C molar	O/C molar	N/C molar	HHV (MJ/kg)
42.1	6.2	5.7	0.4	18.4	1.77	0.33	0.12	20.0

^acalculated by difference

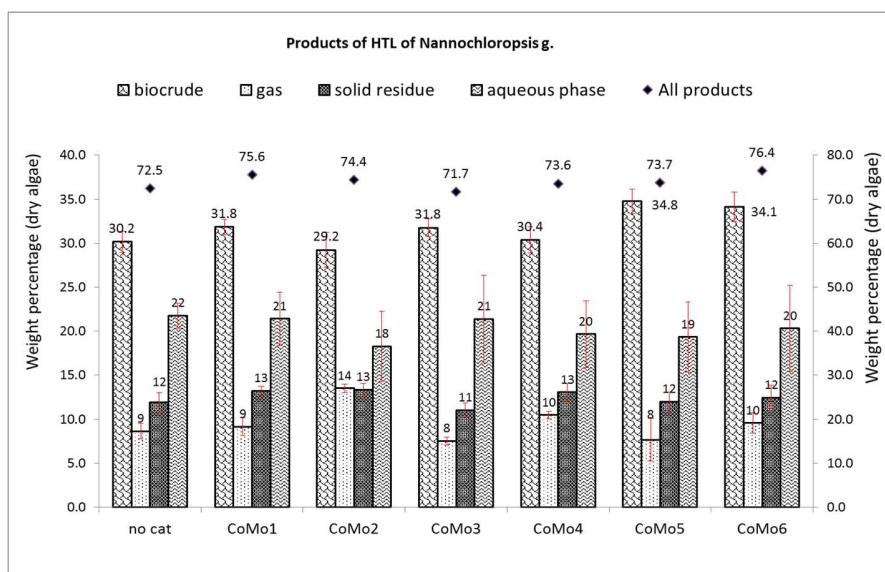


Figure 12. Product distribution for the catalytic HTL of the microalga *Nannochloropsis gaditana*, performed at 375 °C for 15 min, with biomass initial concentration of 10 wt% (dry algae) and catalyst/biomass ratio of 8.4 wt%. Product yields are referred to the initial dry feedstock. For comparison, the results of the test without catalyst are also reported.

All catalysts prepared by impregnation method (CoMo1, CoMo2 and CoMo3) gave biocrude yields close to that obtained in the absence of added catalyst. This could be due to the limited hydrothermal stability that these catalytic systems showed in hydrothermal environment. On the other hand, among the three catalysts prepared by the one-pot colloidal approach (CoMo4, CoMo5 and CoMo6), the one with lower metal loading (CoMo4, with 0.6 wt% Co and 6.4 wt% Mo) exhibited a marginal effect on the biocrude yield, while the two other catalysts with 1.2 wt% Co and 15.2 wt% Mo (CoMo5 and CoMo6) allowed for increasing the biocrude mass yield by about 3.9-4.6%, that is a statistical significant modification with respect to the catalyst-free test (*i.e.* 15% higher). The catalysts prepared with the highest Co and Mo loadings by the one-pot colloidal route were the most effective in enhancing this figure of merit. Interestingly, impregnated catalyst with

the same metal loadings, (CoMo₃), did not induce an analogous gain in biocrude production, even if the hydrothermal stability of this catalyst was found to be quite good with respect to the other impregnated catalysts with lower metal loading (Table 3). For this catalyst, the diffraction peaks of Al₂(MoO₄)₃ and MoO₃ were clearly detectable, indicating formation of large Al₂(MoO₄)₃ and MoO₃ crystallites (see Figure 11).

The catalysts prepared by the one-pot colloidal approach were the focus of the following examination because they were stable under hydrothermal conditions and gave the highest biocrude yields. The elemental composition of biocrude oil obtained with those catalysts, as well as that of non-catalytic test are reported in Table 5. Overall, the catalysts did not cause any change in the biocrude higher heating values (HHV), even at the highest metal loading, but a clear increase in the oil yield was observed. The bio-oil produced under the adopted operating conditions has a high energy density with HHV up to 37 MJ/kg. The total amount of the recovered products accounted for 75% of the initial biomass in all experiments. The obtained yields of gas and solid residue are in the range usually reported in literature for HTL of microalgae at temperature of 350-375 °C.^{82,83,84} The gas phase composition was similar in the absence and in the presence of all tested catalysts. It was mainly constituted of CO₂ (90 mol%), CO (about 5 mol%) and few volumetric percentages of H₂ and CH₄, C₂H₄ and C₂H₆, in agreement with literature.⁸⁵ For what concern the yield in aqueous products, it was found in the range 10-13 wt% that is lower than that reported in the literature for HTL of similar microalgae.⁸⁶ Some authors calculated the aqueous phase yield both as complement to 100 wt% of the quantified gas, bio-oil and solid residue fractions, and after the solvent removal from the aqueous phase through stripping with N₂ for 6 h.⁸⁷ They found a big difference between the two estimations and ascribed it to the presence of water-soluble high volatile organic compounds which were removed during the solvent stripping.

Analogous considerations were reported by Zhou *et al.*⁷⁹, who estimated the water-soluble products after evaporation of water from the aqueous fraction at 65 °C for 12 h. Thus, it seems probable that the missing aliquot to close the mass balance in the product distribution of Figure 12 could be similarly explained as loss of volatile organic compounds during the aqueous phase collection *via* vacuum filtration and during the evaporation of water at 60 °C overnight.

Table 5. Ultimate analysis of the biocrude obtained with HTL of *Nannochloropsis gaditana* at 375 °C, 15 min in the presence of catalysts prepared by the one-pot colloidal approach.

Cat.	C (wt%)	H (wt%)	N (wt%)	S (wt%)	O ^a (wt%)	H/C molar	O/C molar	N/C molar	HHV (MJ/kg)	Yield _{oil} ^b (wt%)	ER% (%)
none	74.9	10.1	3.6	0.3	11.0	1.62	0.11	0.04	37.0	30.2	55.6
CoMo4	73.5	10.0	3.0	0.3	13.2	1.63	0.13	0.03	36.1	30.4	54.7
CoMo5	73.0	10.7	3.0	0.3	13.0	1.76	0.13	0.04	36.7	34.8	63.7
CoMo6	74.6	10.1	3.6	0.3	11.4	1.62	0.11	0.04	36.7	34.1	62.5

^acalculated by difference; ^byield calculated with respect to dry algae (dry basis)

Figure 13 shows the comparison of quantitative GC-MS analyses of biocrude obtained with the two best catalysts which gave the highest yield in bio-oil, *i.e.* CoMo5 and CoMo6, compared to the test without catalyst. Six C14-C18 fatty acids (FAs) were detected and quantified using standards. They are generated by the triglyceride hydrolysis, which is a fast chemical step in the presence of hot water at operation temperature adopted in the study.⁸⁸ Fatty acids could transform into hydrocarbons *via* hydrodeoxygenation (HDO) or hydrodecarboxylation (HDC) processes, forming water or CO₂, respectively,⁸⁹ both of these processes reducing the oxygen content in the bio-oil.

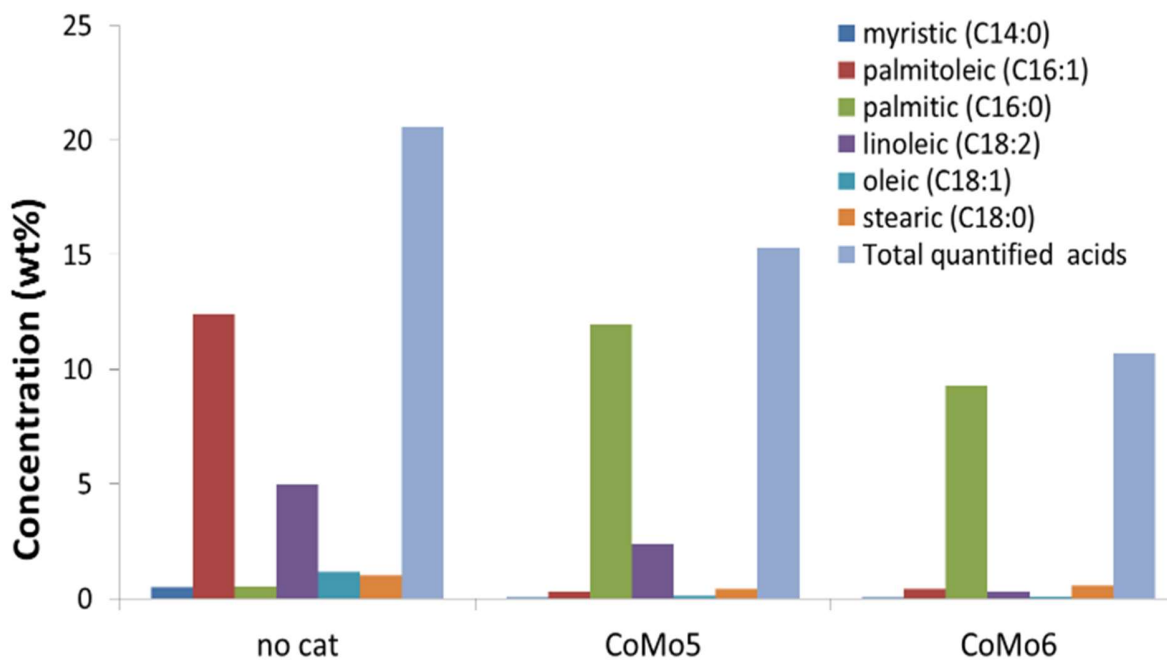


Figure 13. Quantification *via* GC-MS of six common fatty acids in algal biomass, present in the bio-oil obtained with the two catalysts which gave the higher oil yield (CoMo5 and CoMo6), compared with the test without catalyst (no cat). C14:0 = myristic acid; C16:1 = palmitoleic acid; C16:0 = palmitic acid; C18:2 = linoleic acid; C18:1 = oleic acid; C18:0 = stearic acid.

In comparison with conventional fossil fuels, bio-oil contains much higher oxygen contents, which dramatically decrease its heating value and may cause other undesirable effects, such as high viscosity, instability and corrosion. Removal of oxygen is therefore critical for bio-oil upgrading. In the presence of the two catalysts, a reduction of the amount of detected fatty acids was observed with respect to the bio-oil obtained with the thermal test, indicating an improvement in the oxygen removal activity. In particular, the cumulative amount of detected FAs was lower with CoMo6 in comparison with CoMo5 indicating higher activity of this catalyst for *in-situ* partial upgrading of the obtained bio-oil.

By the GC-MS analyses, we also detected the presence of hydrocarbons in the analyzed samples. Quite interestingly, the ratio between the cumulative area of peaks assigned to hydrocarbons and that of fatty acids increased in the order CoMo6>CoMo5>no catalyst (Table 6), which could be another indication of a better capability of higher loading catalyst prepared by one-pot approach to remove oxygen from biocrude.

Table 6. Ratio between cumulative Area percent of the peaks assigned to hydrocarbons (A) and to fatty acids (B), respectively.

Cat	A/B
none	0.3
CoMo5	0.45
CoMo6	1.73

In Table 5 is shown the Energy Recovery (ER) obtained in the experiments, defined by the following equations⁹⁰:

$$ER (\%) = \frac{HHV \text{ of biocrude oil} \times \text{mass yield of biocrude oil}}{HHV \text{ of feedstock}} \times 100$$

This parameter indicates how the process is effective in concentrating the energy content of the initial biomass feedstock in the obtained bio-oil. As both the yield and the HHV of the bio-oil are taken into account, this parameter highlights the role of the catalyst in orienting the process toward the formation of more energetic compounds in the obtained bio-oil. We found that the catalyst obtained through the one-pot colloidal approach at high active metals loadings could yield an

energy recovery of 63-64% that is much higher than that obtained from HTL processes performed in the absence of catalyst.

Nevertheless, it is important to emphasize that the hydrothermal liquefaction of microalga is still in a developing stage and further process improvement is needed for increasing biocrude oil yield and quality. Moreover, the separation of the catalyst from the solid residues (typically ashes) and its reusability are still important factors that need to be evaluated in the microalga biorefinery processes. Another important aspect is the experimental set-up which should also be modified to protect the catalyst from fouling and be sure that there is a good contact with the organic molecules and the aqueous phase. This study must be performed with a modified experimental set-up to decouple the effect of the phase behavior of the reaction system from the catalytic effects. Indeed, at reaction conditions, different phases are generated inside an unstirred reactor, *i.e.* an oil-rich phase with suspended solid at the bottom, a water-rich phase with suspended solids in the middle and a gas-phase at the top. We think that experimental outcomes are dependent not only on the catalyst nature but also on the relative amounts of aforementioned phases and on their contact with the catalyst. To remove these sources of uncertainty, we are currently working on changing the batch reaction system in a two-step continuous process in which the first one is a thermally activated HTL in a well-stirred CSTR connected in sequence with a fixed bed reactor loaded with the catalyst in which the biocrude-rich phase is up-graded.

Conclusions

In this work, two experimental procedures for cyclodextrin-assisted synthesis of CoMo-based catalysts for HTL of microalgae were proposed and compared. Catalysts were extensively

characterized by different techniques such as diffuse reflectance UV-visible spectroscopy, X-ray diffraction, N₂-adsorption-desorption and H₂-temperature programmed reduction. Results showed that both methods allow preparation of mesoporous structures with high surface area (300-450 m²/g). Catalysts prepared by the one-pot colloidal approach exhibited high stability, even at low metal loadings, after exposure to hydrothermal environment. Differently, the stability of catalysts prepared by impregnation was affected by the metal loading. Catalyst characterizations suggested that this behavior could be attributed to a better dispersion and incorporation of the active catalytic species into the alumina support framework. In particular, the incorporation of tetrahedral coordinated divalent Co species (cobalt aluminate phase CoAl₂O₄, spinel) was found to occur more effectively for catalysts prepared *via* the one-pot method. Results of microalgae HTL tests showed that impregnated catalysts had almost no effect on the performances of the process in comparison with the catalyst-free test. Interesting results were obtained with the two catalysts prepared by the one-pot approach with the highest Co and Mo loadings. Thus, the combination of higher yield and higher heating value (HHV) of the obtained biocrude led to a 13% enhancement of the biomass energy recovery (ER) into the biocrude with respect to the catalyst-free test. Moreover, the nature of the block copolymer used during the CoMo/ γ -Al₂O₃ preparation was also found to affect the catalyst performance. Thus, the ability of pH-sensitive Tetronic T90R4 to interact through its positively charged amino groups with the negatively charged [Co₂Mo₇O₂₄]²⁻ complex was beneficial in the oxygen removal efficiency from biocrude. The proposed one-pot cyclodextrin-assisted approach presented in this study gave promising results toward the preparation of hydrothermally stable catalytic systems and can be used to prepare many other composites of technological importance.

Conflicts of interest

There are no conflicts to declare.

AUTHOR INFORMATION

Corresponding Authors:

*E-mail: rudina.bleta@univ-artois.fr

*E-mail: alessandro.galia@unipa.it

Acknowledgements

The financial support of MIUR under project PRIN 2010-2011 2010H7PXLC_005 and of European Commission under project STAGE-STE FP7 Cooperation 609837 is gratefully acknowledged. The European Regional Development Fund (ERDF), the Conseil Regional du Haut de France, the CNRS and the Ministère de l'Education Nationale de l'Enseignement Supérieur et de la Recherche are acknowledged for funding of the X-ray diffractometer.

References

- [1] Besson, M.; Gallezot, P.; Pinel, C., Conversion of Biomass into Chemicals over Metal Catalysts. *Chem. Rev.* **2014**, *114*, 1827-1870.
- [2] Lin, Y. C.; Huber, G. W., The critical role of heterogeneous catalysis in lignocellulosic biomass conversion. *Energy Environ. Sci.* **2009**, *2*, 68-80.
- [3] Wijffels, R. H.; Barbosa, M. J., An outlook on microalgal biofuels. *Science* **2010**, *329*, 796-799.

-
- [4] Akhtar, J.; Amin, N. A. S., A review on process conditions for optimum bio-oil yield in hydrothermal liquefaction of biomass. *Renew. Sustain. Energy Rev.* **2011**, *15*, 1615-1624.
- [5] Albrecht, K. O.; Zhu, Y.; Schmidt, A. J.; Billing, J. M. Hart, T. R.; Jones, S. B.; Maupin, G.; Hallen, R.; Ahrens, T.; Anderson, D., Impact of heterotrophically stressed algae for biofuel production via hydrothermal liquefaction and catalytic hydrotreating in continuous-flow reactors. *Algal Research* **2016**, *14*, 17-27.
- [6] Arturi, K. R.; Kucheryavskiy, S.; Søggaard, E. G., Performance of hydrothermal liquefaction (HTL) of biomass by multivariate data analysis, *Fuel Processing Technology* **2016**, *150*, 94-103.
- [7] Tian, C.; Li, B.; Liu, Z.; Zhang, Y.; Lu, H., Hydrothermal liquefaction for algal biorefinery: A critical review, *Renew. Sust. Energ. Rev.* **2014**, *38*, 933-950.
- [8] López Barreiro, D.; Prins, W.; Ronsse, F.; Brilman, W., Hydrothermal liquefaction (HTL) of microalgae for biofuel production: State of the art review and future prospects, *Biomass Bioenergy* **2013**, *53*, 113-127.
- [9] Biller, P.; Ross, A. B., Hydrothermal processing of algal biomass for the production of biofuels and chemicals, *Biofuels* **2012**, *3*, 603-623.
- [10] Kruse, A.; Dahmen, N., Water-A magic solvent for biomass conversion. *J. Supercrit. Fluids* **2015**, *96*, 36-45.
- [11] Elliott, D. C.; Beckman, D.; Bridgwater, A. V.; Diebold, J. P.; Gevert, S. B.; Solantausta, Y. Developments in direct thermochemical liquefaction of biomass: 1983-1990. *Energy Fuels* **1991**, *5*(3), 399-410.
- [12] Elliott, D. C. Historical developments in hydroprocessing bio-oils. *Energy Fuels* **2007**, *21*(3), 1792-1815.

-
- [13] Duan, P.; Savage, P. E., Hydrothermal liquefaction of a microalga with heterogeneous catalysts. *Ind. Eng. Chem. Res.* **2011**, *50*, 52-61.
- [14] Yu, G.; Zhang, Y.; Guo, B.; Funk, T.; Schideman, L., Nutrient flows and quality of bio-crude oil produced via catalytic hydrothermal liquefaction of low-lipid microalgae. *Bioenergy Res.* **2014**, *7*, 1317-1328.
- [15] Biller, P.; Riley, R.; Ross, A. B., Catalytic hydrothermal processing of microalgae: decomposition and upgrading of lipids. *Bioresour. Technol.* **2011**, *102*, 4841-4848.
- [16] Li, J.; Wang, G.; Gao, C.; Lv, X.; Wang, Z.; Liu, H., *Energy and Fuels* **2013**, *27*, 5207-5214.
- [17] Xu, Y.; Zheng, X.; Yu, H.; Hu, X., Hydrothermal liquefaction of *Chlorella pyrenoidosa* for bio-oil production over Ce/HZSM-5. *Bioresour. Technol.* **2014**, *156*, 1-5.
- [18] Egesa, D.; Chuck, C. J.; Plucinski, P.; Multifunctional role of magnetic nanoparticles in efficient microalgae separation and catalytic hydrothermal liquefaction. *ACS Sustainable Chem. Eng.* **2018**, *6*, 991-999.
- [19] Galadima, A.; Muraza, O; Hydrothermal liquefaction of algae and bio-oil upgrading into liquid fuels: Role of heterogeneous catalysts. *Renew. Sust. Energ. Rev.* **2018**, *81*, 1037-1048.
- [20] Ravenelle, R. M.; Copeland, J. R.; Van Pelt, A. H.; Crittenden, J.C.; Sievers, C., Stability of Pt/ γ -Al₂O₃ catalysts in model biomass solutions. *Top. Catal.* **2012**, *55*, 162-174.
- [21] Ravenelle, R. M.; Copeland, J. R.; Kim, W. G.; Crittenden, J. C.; Sievers, C., Structural changes of γ -Al₂O₃-supported catalysts in hot liquid water. *ACS Catal.* **2011**, *1*, 552-561.
- [22] Copeland, J. R.; Shi, X. R.; Sholl, D. S.; Sievers, C., Surface interactions of C₂ and C₃ polyols with γ -Al₂O₃ and the role of coadsorbed water. *Langmuir* **2013**, *29*, 581-593.

-
- [23] Jongerius, A. L.; Copeland, J. R.; Shiou Foo, G.; Hofmann, J. P.; Bruijninx, P. C. A.; Sievers, C.; Weckhuysen, B. M., Stability of Pt/ γ -Al₂O₃ catalysts in lignin and lignin model compound solutions under liquid phase reforming reaction conditions. *ACS Catal.* **2013**, *3*, 464-473.
- [24] Szejtli, J., Introduction and general overview of cyclodextrin chemistry. *Chem. Rev.* **1998**, *98*, 1743-1753.
- [25] Breslow, R.; Dong, S. D., Biomimetic reactions catalyzed by cyclodextrins and their derivatives. *Chem. Rev.* **1998**, *98*, 1997-2011.
- [26] Bleta, R.; Noël, S.; Addad, A.; Ponchel, A.; Monflier, E., Mesoporous RuO₂/TiO₂ composites prepared by cyclodextrin-assisted colloidal self-assembly: towards efficient catalysts for the hydrogenation of methyl oleate. *RSC Adv.* **2016**, *6*, 14570-14579.
- [27] Lannoy, A.; Bleta, R.; Machut-Binkowski, C.; Addad, A.; Monflier, E.; Ponchel, A. Cyclodextrin-directed synthesis of gold-modified TiO₂ materials and evaluation of their photocatalytic activity in the removal of a pesticide from water: Effect of porosity and particle size. *ACS Sustainable Chem. Eng.* **2017**, *5*, 3623-3630.
- [28] Yoldas, B. E., Alumina sol preparation from alkoxides. *Am. Ceram. Soc. Bull.* **1975**, *54*, 289-290.
- [29] Brunauer, S.; Emmett, P. H.; Teller, E., Adsorption of gases in multimolecular layers. *J. Am. Chem. Soc.* **1938**, *60*, 309-319.
- [30] Barrett, E.P.; Joyner, L.G.; Halenda, P.P., The determination of pore volume and area distributions in porous substances. I. Computations from nitrogen isotherms. *J. Amer. Chem. Soc.* **1951**, *61*, 373-380.

-
- [31] Channiwala, S. A.; Parikh, P. P., A unified correlation for estimating HHV of solid, liquid and gaseous fuels. *Fuel* **2002**, *81*, 1051-1063.
- [32] Bleta, R.; Machut, C.; Léger, B.; Monflier, E.; Ponchel, A., Coassembly of block copolymer and randomly methylated β -cyclodextrin: from swollen micelles to mesoporous alumina with tunable pore size. *Macromolecules* **2013**, *46*, 5672-5683.
- [33] Bleta, R.; Machut, C.; Léger, B.; Monflier, E.; Ponchel, A., Investigating the effect of randomly methylated β -cyclodextrin/block copolymer molar ratio on the template-directed preparation of mesoporous alumina with tailored porosity. *J. Incl. Phenom. Macrocycl. Chem.* **2014**, *80*, 323-335.
- [34] Jean-Marie, A.; Griboval-Constant, A.; Khodakov, A. Y.; Monflier, E.; Diehl, F., β -Cyclodextrin for design of alumina supported cobalt catalysts efficient in Fischer-Tropsch synthesis. *Chem. Commun.* **2011**, *47*, 10767-10769.
- [35] Bergwerff, J. A.; Visser, T.; Weckhuysen, B.M., On the interaction between Co- and Mo-complexes in impregnation solutions used for the preparation of Al_2O_3 -supported HDS catalysts: A combined Raman/UV-vis-NIR spectroscopy study. *Catalysis Today* **2008**, *130*, 117-125.
- [36] Long, D.; Kögerler, P.; Farrugia, L. J.; Cronin, L., Reactions of a $\{\text{Mo}_{16}\}$ -type polyoxometalate cluster with electrophiles: a synthetic, theoretical and magnetic investigation. *Dalton Trans.* **2005**, 1372-1380.
- [37] Alvarez-Lorenzo, C.; Gonzalez-Lopez, J.; Fernandez-Tarrio, M.; Sandez-Macho, I.; Concheiro, A., Tetronic micellization, gelation and drug solubilization: Influence of pH and ionic strength. *Eur. J. Pharm. Biopharm.* **2007**, *66*, 244-252.
- [38] Larrañeta, E.; Ramón Isasi, J., Phase behavior of reverse poloxamers and poloxamines in water. *Langmuir* **2013**, *29*, 1045-1053.

-
- [39] Basak, R.; Bandyopadhyay, R., Encapsulation of hydrophobic drugs in Pluronic F127 micelles: Effects of drug hydrophobicity, solution temperature, and pH. *Langmuir* **2013**, *29*, 4350-4356.
- [40] Plestil, J.; Pospisil, H.; Sikora, A.; Krakovsky, I.; Kuklin, A., Small-angle neutron scattering and differential scanning calorimetry study of associative behaviour of branched poly(ethylene oxide)/poly(propylene oxide) copolymer in aqueous solution. *J. Appl. Crystallogr.* **2003**, *36*, 970-975.
- [41] Ramirez, J.; Castillo, P.; Cedefio, L.; Cuevas, R.; Castillo, M.; Palacios, J.; Agudo, A. L., Effect of boron addition on the activity and selectivity of hydrotreating CoMo/Al₂O₃ catalysts. *Appl. Catal. A* **1995**, *132*, 317-334.
- [42] Weber, R. S., Effect of local structure on the UV-visible absorption edges of molybdenum oxide clusters and supported molybdenum oxides. *J. Catal.* **1995**, *151*, 470-474.
- [43] Wang, X.; Fang, H.; Zhao, Z.; Duan, A.; Xu, C., Effect of promoters on the HDS activity of alumina-supported Co-Mo sulfide catalysts. *RSC Adv.* **2015**, *5*, 99706-99711.
- [44] Du, P.; Zheng, P.; Song, S.; Wang, X.; Zhang, M.; Chi, K.; Xu, C.; Duan, A.; Zhao, Z., Synthesis of a novel micro/mesoporous composite material Beta-FDU-12 and its hydro-upgrading performance for FCC gasoline. *RSC Adv.* **2016**, *6*, 1018-1026.
- [45] Ramirez, J.; Contreras, R.; Castillo, P.; Klimova, T.; Zárate, R.; Luna, R., Characterization and catalytic activity of CoMo HDS catalysts supported on alumina-MCM-41. *Appl. Catal. A* **2000**, *197*, 69-78.
- [46] Zheng, W.; Zou, J., Synthesis and characterization of blue TiO₂/CoAl₂O₄ complex pigments with good colour and enhanced near-infrared reflectance properties. *RSC Adv.* **2015**, *5*, 87932-87939.

-
- [47] Cava, S.; Tebcherani, S. M.; Pianaro, S. A.; Paskocimas, C. A.; Longo, E.; Varela, J. A., Structural and spectroscopic analysis of γ -Al₂O₃ to α -Al₂O₃-CoAl₂O₄ phase transition. *Mater. Chem. Phys.* **2006**, *97*, 102-108.
- [48] Wang, W.; Xie, Z.; Liu, G.; Yang, W., Fabrication of blue-colored zirconia ceramics via heterogeneous nucleation method. *Cryst. Growth Des.* **2009**, *9*, 4373-4377.
- [49] Rangappa, D.; Naka, T.; Kondo, A.; Ishii, M.; Kobayashi, T.; Adschiri, T., Transparent CoAl₂O₄ hybrid nano pigment by organic ligand-assisted supercritical water. *J. Am. Chem. Soc.* **2007**, *129*, 11061-11066.
- [50] Vakrosa, J.; Lycourghiotis, A.; Voyiatzis, G. A.; Siokou, A.; Kordulis, C., CoMo/Al₂O₃-SiO₂ catalysts prepared by co-equilibrium deposition filtration: characterization and catalytic behavior for the hydrodesulphurization of thiophene. *Appl. Catal. B* **2010**, *96*, 496-507.
- [51] Arnoldy, P.; Moulijn, J. A., Temperature-programmed reduction of CoAl₂O₃ catalysts. *J. Catal.* **1985**, *93*, 38-54.
- [52] Tielens, F.; Calatayud, M.; Franco, R.; Recio, J. M.; Pérez-Ramírez, J.; Minot, C., Periodic DFT study of the structural and electronic properties of bulk CoAl₂O₄ spinel. *J. Phys. Chem. B* **2006**, *110*, 988-995.
- [53] Liu, X. M.; Xue, H. X.; Li, X.; Yan, Z. F., Synthesis and hydrodesulfurization performance of hierarchical mesopores alumina. *Catal. Today* **2010**, *158*, 446-451.
- [54] Arnoldy, P.; Franken, M. C.; Scheffer, B.; Moulijn, J. A., Temperature-programmed reduction of CoO/MoO₃/Al₂O₃ catalysts. *J. Catal.* **1985**, *96*, 381-395.
- [55] Rajagopal, S.; Marini, H. J.; Marzari, J. A.; Miranda, R., Silica-alumina-supported acidic molybdenum catalysts-TPR and XRD characterization. *J. Catal.* **1994**, *147*, 417-428.

-
- [56] Qu, L. L.; Zhang, W. P.; Kooyman, P. J.; Prins, R., MAS NMR, TPR, and TEM studies of the interaction of NiMo with alumina and silica-alumina supports. *J. Catal.* **2003**, *215*, 7-13.
- [57] Chen, H.; Adesina, A. A., Improved alkene selectivity in carbon monoxide hydrogenation over silica supported cobalt-molybdenum catalyst. *Appl. Catal. A Gen.* **1994**, *112*, 87-103.
- [58] Rodriguez, J. A.; Chaturvedi, S.; Hanson, J. C.; Brito, J. L. J., Reaction of H₂ and H₂S with CoMoO₄ and NiMoO₄: TPR, XANES, time-resolved XRD, and molecular-orbital studies. *Phys. Chem. B* **1999**, *103*, 770-781.
- [59] Lopez Cordero, R.; Gil Llambias, F.J.; Lopez Agudo, A., Temperature-programmed reduction and zeta potential studies of the structure of Mo/O₃Al₂O₃ and Mo/O₃SiO₂ catalysts effect of the impregnation pH and molybdenum loading. *Appl. Catal.* **1991**, *74*, 125-136.
- [60] MacDonald, D. D.; Butler, P., The thermodynamics of the aluminium-water system at elevated temperatures. *Corros. Sci.* **1973**, *13*, 259-274.
- [61] Ravenelle, R. M.; Diallo, F. Z.; Crittenden, J. C.; Sievers, C., Effects of metal precursors on the stability and observed reactivity of Pt/ γ -Al₂O₃ catalysts in aqueous phase reactions. *ChemCatChem* **2012**, *4*, 492-494.
- [62] Luo, N.; Fu, X.; Cao, F.; Xiao, T.; Edwards, P. P., Glycerol aqueous phase reforming for hydrogen generation over Pt catalyst—Effect of catalyst composition and reaction conditions. *Fuel* **2008**, *87*, 3483-3489.
- [63] Ketchie, W. C.; Maris, E. P.; Davis, R. J., In-situ X-ray absorption spectroscopy of supported Ru catalysts in the aqueous phase. *Chem. Mater.* **2007**, *19*, 3406-3411.
- [64] McHale, J. M.; Auroux, A.; Perrotta, A. J.; Navrotsky, A., Surface energies and thermodynamic phase stability in nanocrystalline aluminas., *Science* **1997**, *277*(5327), 788-791.

-
- [65] Lefèvre, G.; Duc, M.; Lepeut, P.; Caplain, R.; Fédoroff, M., Hydration of γ -alumina in water and its effects on surface reactivity. *Langmuir* **2002**, *18*, 7530-7537.
- [66] Castro, R. H. R.; Ushakov, S. V.; Gengembre, L.; Gouvêa, D.; Navrotsky, A., Surface energy and thermodynamic stability of γ -alumina: Effect of dopants and water. *Chem. Mater.* **2006**, *18*, 1867-1872.
- [67] Sing, K. S. W., Reporting physisorption data for gas/solid systems with special reference to the determination of surface area and porosity. *Pure and Applied Chemistry* **1982**, *54*, 2201-2218.
- [68] Bleta, R.; Jaubert, O.; Gressier, M.; Menu, M. J., Rheological behaviour and spectroscopic investigations of cerium-modified AlO(OH) colloidal suspensions. *J. Colloid. Interf. Sci.* **2011**, *363*, 557-565.
- [69] Krokidis, X.; Raybaud, P.; Gobichon, A. E.; Rebours, B.; Euzen, P.; Toulhoat, H., Theoretical study of the dehydration process of boehmite to γ -alumina. *J. Phys. Chem. B* **2001**, *105*, 5121-5130.
- [70] Alphonse, P.; Courty, M., Structure and thermal behavior of nanocrystalline boehmite. *Thermochimica. Acta* **2005**, *425*, 75-89.
- [71] Raybaud, P.; Digne, M.; Iftimie, R.; Wellens, W.; Euzen, P.; Toulhoat, H., Morphology and surface properties of boehmite (γ -AlOOH): a density functional theory study. *J. Catal.* **2001**, *201*, 236-246.
- [72] Bleta, R.; Alphonse, P.; Pin, L.; Gressier, M.; Menu, M. J., An efficient route to aqueous phase synthesis of nanocrystalline γ -Al₂O₃ with high porosity: from stable boehmite colloids to large pore mesoporous alumina. *J Colloid Interface Sci.* **2012**, *367*, 120-128.

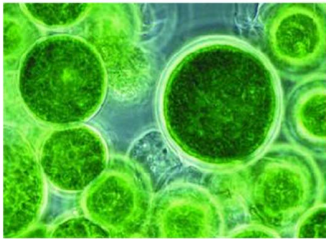
-
- [73] Dandapat, A.; De, G., Host-mediated synthesis of cobalt aluminate/ γ -alumina nanoflakes: a dispersible composite pigment with high catalytic activities. *ACS Appl. Mater. Interfaces* **2012**, *4*, 228-234.
- [74] Maglia, F.; Gennari, S.; Buscaglia, V., Energetics of aluminum vacancies and incorporation of foreign trivalent ions in γ -Al₂O₃: An atomistic simulation study. *J. Am. Ceram. Soc.* **2008**, *91*, 283-290.
- [75] Thormählen, P.; Fridell, E.; Cruise, N.; Skoglundh, M.; Palmqvist, A., The influence of CO₂, C₃H₆, NO, H₂, H₂O or SO₂ on the low-temperature oxidation of CO on a cobalt-aluminate spinel catalyst (Co_{1.66}Al_{1.34}O₄). *Appl. Catal. B: Env.* **2001**, *31*, 1-12.
- [76] Budroni, G.; Corma, A.; García, H.; Primo, A., Pd nanoparticles embedded in sponge-like porous silica as a Suzuki-Miyaura catalyst: Similarities and differences with homogeneous catalysts. *J. Catal.* **2007**, *251*, 345-353.
- [77] Garcia-Martinez, J.; Linares, N.; Sinibaldi, S.; Coronado, E.; Ribera, A., Incorporation of Pd nanoparticles in mesostructured silica. *Microporous and Mesoporous Materials* **2009**, *117*, 170-177.
- [78] Linares, N.; Serrano, E.; Rico, M.; Mariana Balu, A.; Losada, E.; Luque, R.; Garcia-Martinez, J., Incorporation of chemical functionalities in the framework of mesoporous silica. *Chem. Commun.* **2011**, *47*, 9024-9035.
- [79] Zhou, D.; Zhang, L.; Zhang, S.; Fu, H.; Chen, J., Hydrothermal liquefaction of macroalgae *Enteromorpha prolifera* to bio-oil. *Energy and Fuels* **2010**, *24*, 4054-4061.

-
- [80] Alba, L.G.; Torri, C.; Samorì, C.; van der Spek, J.; Fabbri, D.; Kersten, S. R. A.; Brilman, Derk W. F., Hydrothermal treatment (HTT) of microalgae: Evaluation of the process as conversion method in an algae biorefinery concept, *Energy Fuels* **2012**, *26*, 642-657.
- [81] Johnson, J. W.; Norton, D., Critical phenomena in hydrothermal systems: state, thermodynamic, electrostatic, and transport properties of H₂O in the critical region. *American Journal of Science* **1991**, *291*, 541-648.
- [82] Valdez, P. J.; Dickinson, J. G.; Savage, P. E., Characterization of product fractions from hydrothermal liquefaction of *Nannochloropsis* sp. and the influence of solvents. *Energy and Fuels* **2011**, *25*, 3235-3243.
- [83] Jena, U.; Das, K. C.; Kastner, J. R., Effect of operating conditions of thermochemical liquefaction on biocrude production from *Spirulina platensis*. *Bioresour. Technol.* **2011**, *102*, 6221-6229.
- [84] Neveux, N.; Yuen, A. K. L.; Jazrawi, C.; Magnusson, M.; Haynes, B. S.; Masters, A. F.; Montoya, A.; Paul, N. A.; Maschmeyer, T.; de Nys, R., Biocrude yield and productivity from the hydrothermal liquefaction of marine and freshwater green macroalgae. *Bioresour. Technol.* **2014**, *155*, 334-341.
- [85] Chen, Y.; Zhao, N.; Wu, Y.; Wu, K.; Wu, X.; Liu, J.; Yang, M., Distributions of organic compounds to the products from hydrothermal liquefaction of microalgae. *Environ. Prog. Sustain. Energy* **2017**, *36*, 259-268.
- [86] López Barreiro, D.; Samorì, C.; Terranella, G.; Hornung, U.; Kruse, A.; Prins, W., Assessing microalgae biorefinery routes for the production of biofuels via hydrothermal liquefaction. *Bioresour. Technol.* **2014**, *174*, 256-265.

-
- [87] Valdez, P. J.; Nelson, M. C.; Wang, H. Y.; Lin, X. N.; Savage, P. E., Hydrothermal liquefaction of *Nannochloropsis* sp.: Systematic study of process variables and analysis of the product fractions. *Biomass and Bioenergy* **2012**, *46*, 317-331.
- [88] Alenezi, R.; Baig, M.; Wang, J.; Santos, R.; Leeke, G. A., Continuous flow hydrolysis of sunflower oil for biodiesel. *Energy Sources, Part A Recover. Util. Environ. Eff.* **2010**, *32*, 460-468.
- [89] Galadima, A.; Muraza, O. J., Zeolite catalysts in upgrading of bioethanol to fuels range hydrocarbons: A review. *Ind. Eng. Chem.* **2015**, *31*, 1-14.
- [90] Jena, U.; Das, K. C.; Kastner, J. R., Comparison of the effects of Na_2CO_3 , $\text{Ca}_3(\text{PO}_4)_2$, and NiO catalysts on the thermochemical liquefaction of microalga *Spirulina platensis*. *Appl. Energy* **2012**, *98*, 368-375.

Table of Contents Graphic

Microalgae



CoMo/ γ -Al₂O₃



Hydrothermal
liquefaction

Biocrude Oil

- high biocrude yield: 34.1%
- high energy recovery: 62.5%